

# Gravitational waves and neutron stars

Jo van den Brand, Nikhef and Maastricht University, [jo@nikhef.nl](mailto:jo@nikhef.nl)

EINN 2019, Paphos, November 1, 2019



LIGO  
Scientific  
Collaboration



# Gravity

Gravity is the least understood fundamental interaction with many open questions. Should we not now investigate general relativity experimentally, in ways it was never tested before?

## Gravity

- Main organizing principle in the Universe
  - Structure formation
- Most important open problems in contemporary science
  - Acceleration of the Universe is attributed to Dark Energy
  - Standard Model of Cosmology features Dark Matter
  - Or does this signal a breakdown of general relativity?

## Large world-wide intellectual activity

- Theoretical: combining GR + QFT, cosmology, ...
- Experimental: astronomy (CMB, Euclid, LSST), particle physics (LHC), Dark Matter searches (Xenon1T), ...



## Gravitational waves

- Dynamical part of gravitation, all space is filled with GW
- Ideal information carrier, almost no scattering or attenuation
- The entire universe has been transparent for GWs, all the way back to the Big Bang

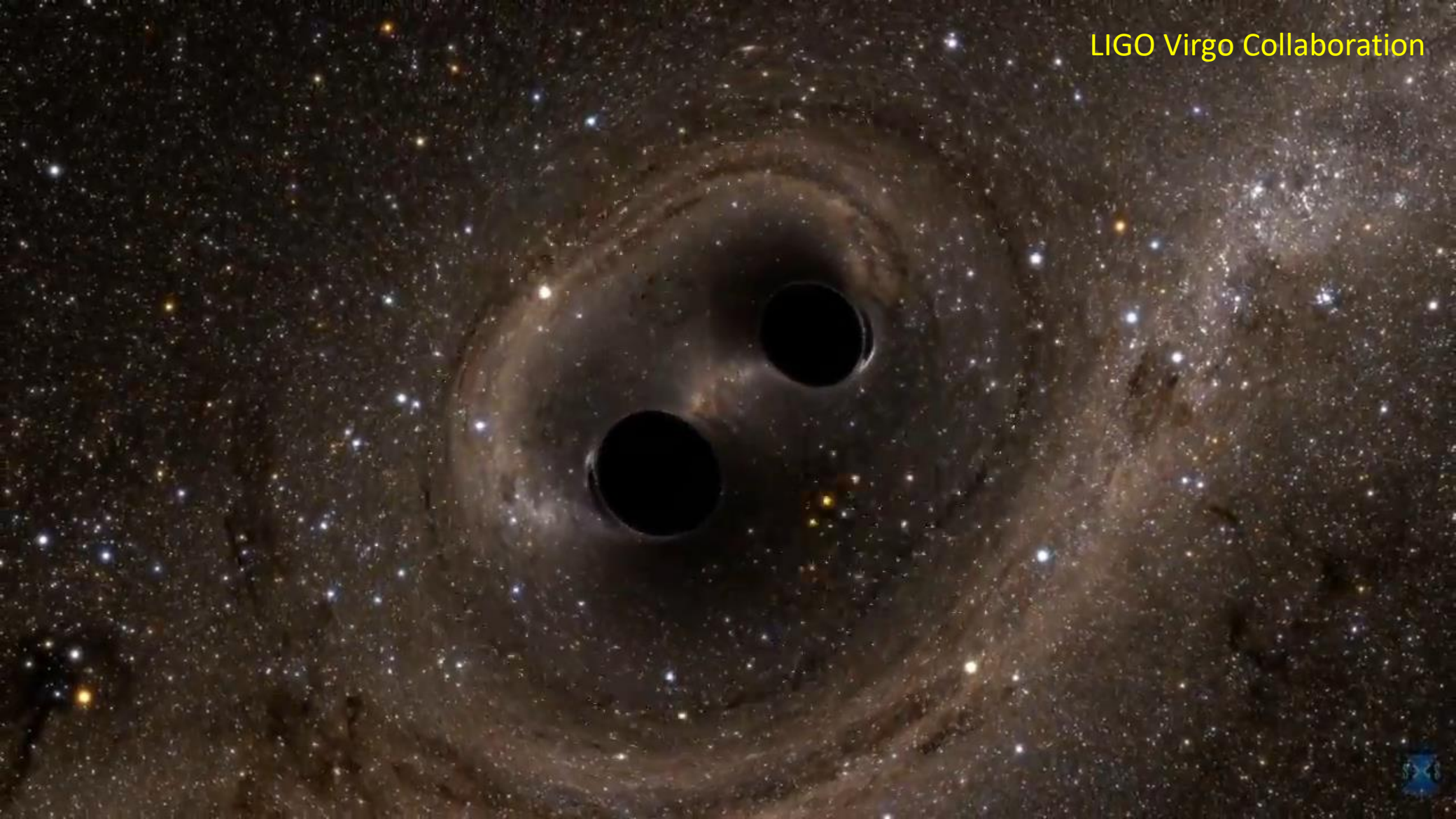
## Gravitational wave science can impact

- Fundamental physics: black holes, spacetime, horizons, matter under extreme conditions
- Cosmology: Hubble parameter, Dark Matter, Dark Energy

# Event GW150914

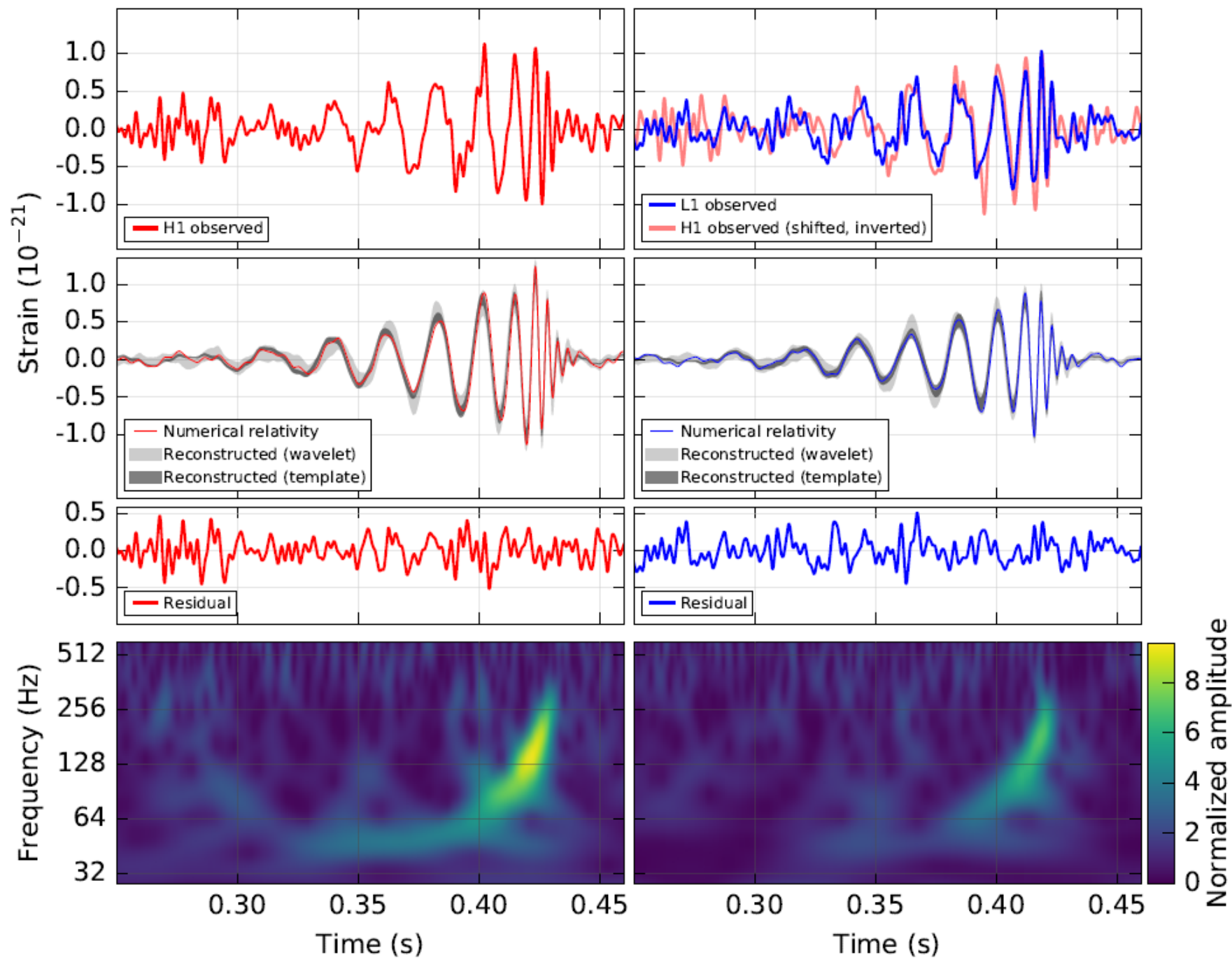
On September 14, 2015 we detected with the LIGO detectors for the first time gravitational waves (vibrations in the fabric of space and time) from the collision of two black holes

LIGO Virgo Collaboration



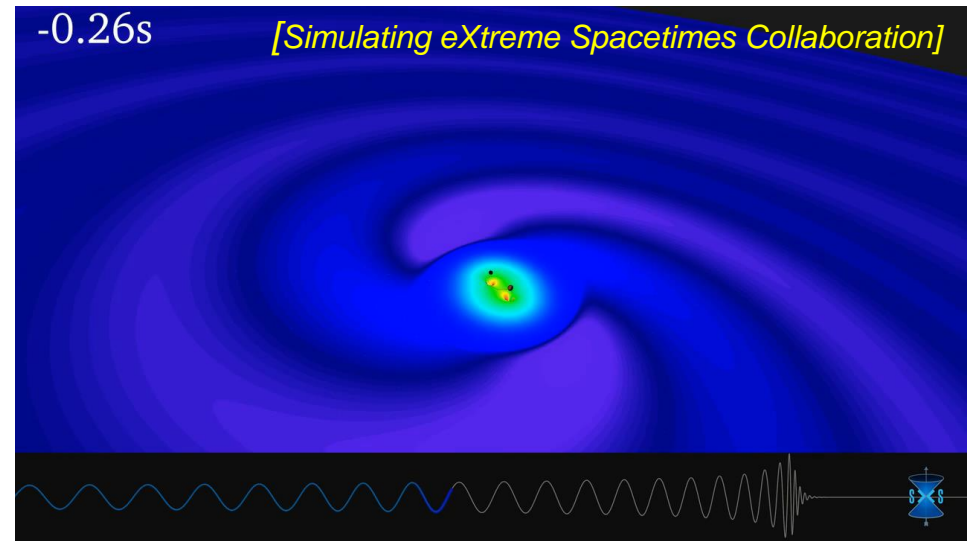
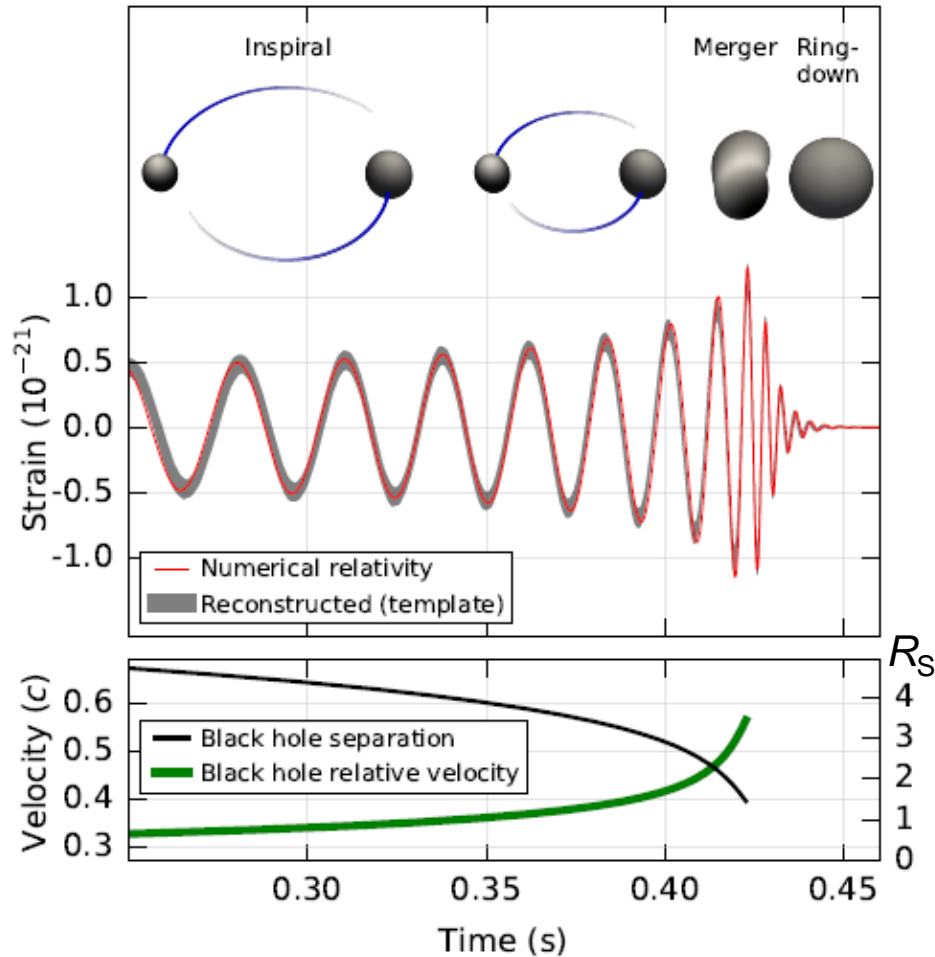
Hanford, Washington (H1)

Livingston, Louisiana (L1)



# Binary black hole merger GW150914

The system will lose energy due to emission of gravitational waves. The black holes get closer and their velocity speeds up. Masses and spins can be determined from inspiral and ringdown phase



- Chirp  $\dot{f} \approx f^{11/3} M_S^{5/3}$
  - Maximum frequency  $f_{\text{ISCO}} = \frac{1}{6^{3/2} \pi M}$
  - Orbital phase (post Newtonian expansion)
- $$\Phi(v) = \left(\frac{v}{c}\right)^{-5} \sum_{n=0}^{\infty} \left[ \varphi_n + \varphi_n^{(l)} \ln\left(\frac{v}{c}\right) \right] \left(\frac{v}{c}\right)^n$$
- Strain  $h \approx \frac{M_S^{5/3} f^{2/3}}{r} = \frac{\dot{f}}{r f^3}$

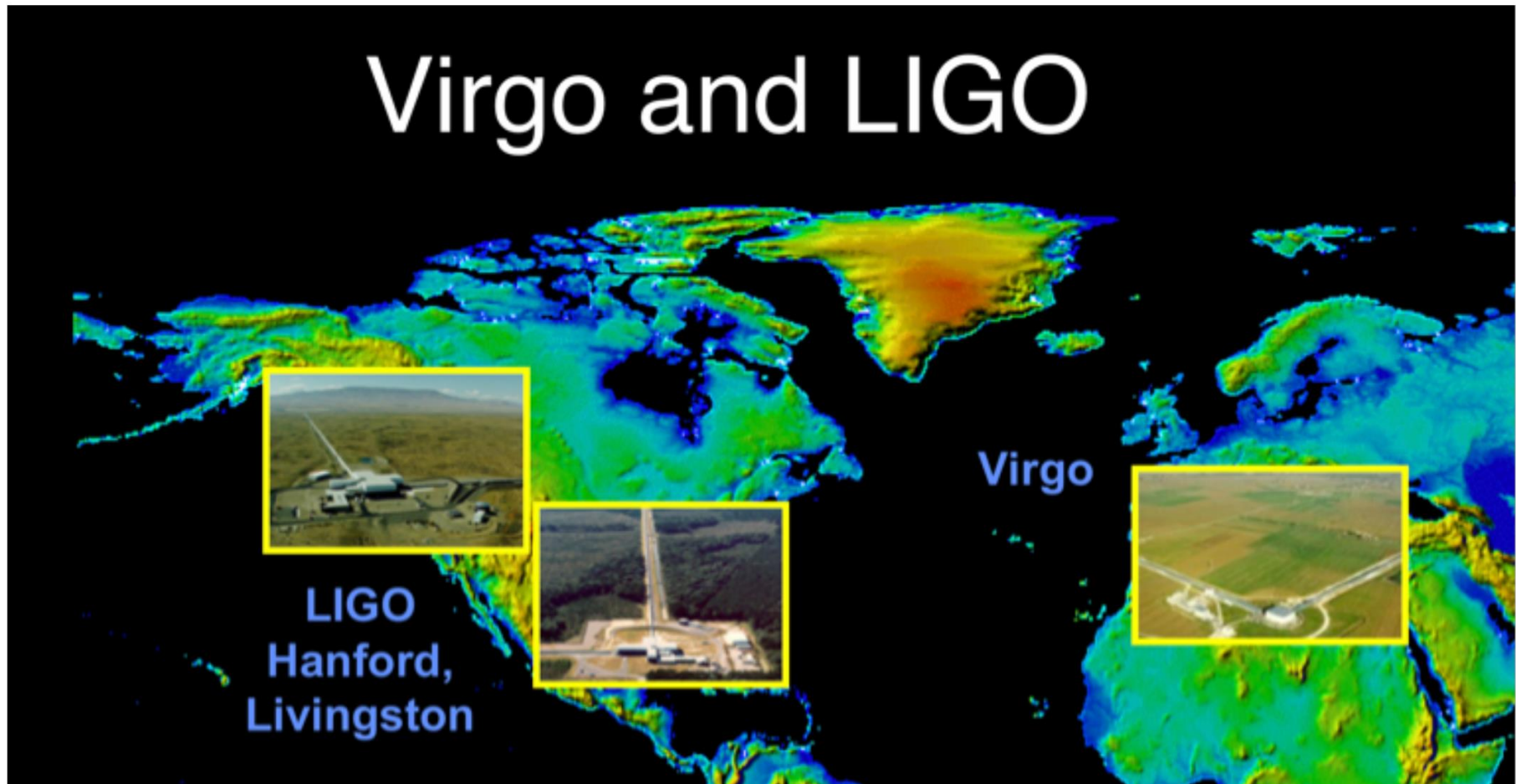
# LIGO and Virgo

Observe together as a Network of GW detectors. LVC have integrated their data analysis

LIGO and Virgo have coordinated data taking and analysis, and release joint publications

LIGO and Virgo work under an MOU already for more than a decade

KAGRA in Japan is expected to join in 2019



# Virgo Collaboration

Virgo is a European collaboration with 482 members, 360 authors, and 96 institutes

Advanced Virgo (AdV) and AdV+: upgrades of the Virgo interferometric detector

Participation by scientists from France, Italy, Belgium, The Netherlands, Poland, Hungary, Spain, Germany

- Institutes in Virgo Steering Committee

- |                       |                         |                         |                                  |
|-----------------------|-------------------------|-------------------------|----------------------------------|
| - APC Paris           | - INFN Perugia          | - LAPP Annecy           | - RMKI Budapest                  |
| - ARTEMIS Nice        | - INFN Pisa             | - LKB Paris             | - UCLouvain, Uliege,<br>UAntwerp |
| - IFAE Barcelona      | - INFN Roma Sapienza    | - LMA Lyon              | - Univ. of Barcelona             |
| - ILM and Navier      | - INFN Roma Tor Vergata | - Maastricht University | - University of Sannio           |
| - INFN Firenze-Urbino | - INFN Trento-Padova    | - Nikhef Amsterdam      | - Univ. of Valencia              |
| - INFN Genova         | - IPHC Strassbourg      | - POLGRAW(Poland)       | - University of Jena             |
| - INFN Napoli         | - LAL Orsay ESPCI Paris | - University Nijmegen   |                                  |

Advanced Virgo project has been formally completed on July 31, 2017

Part of the international network of 2nd generation detectors

Joined the O2 run on August 1, 2017

LIGO and Virgo running of O3



# Scientific achievements: properties of binary systems

“GWTC-1: A Gravitational-Wave Transient Catalog of Compact Binary Mergers Observed by LIGO and Virgo during the First and Second Observing Runs”, LIGO Virgo Collaboration, [arXiv:1811.12907](https://arxiv.org/abs/1811.12907)

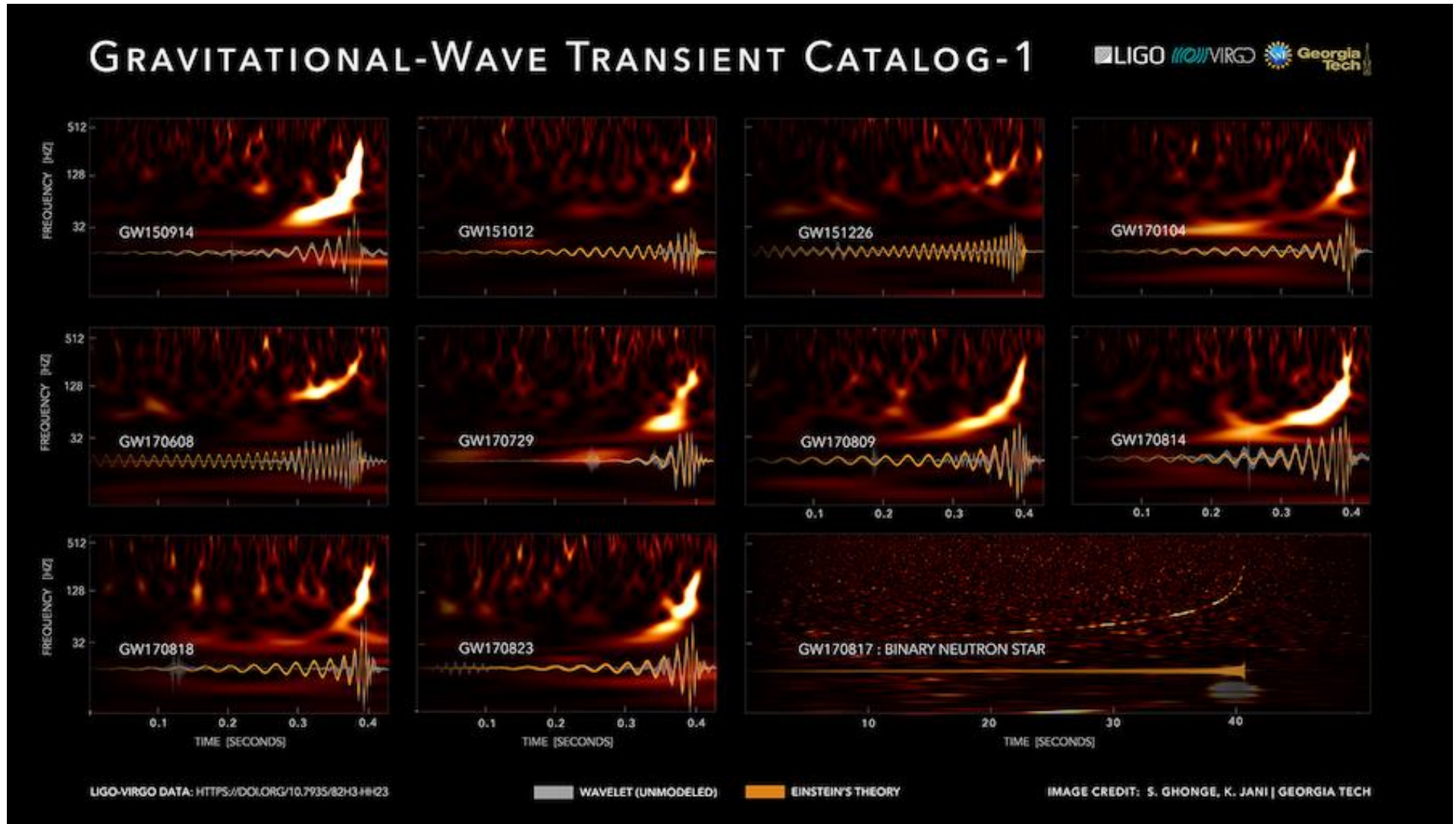


# Table of O1 and O2 triggers with source properties

See [arXiv:1811.12907](https://arxiv.org/abs/1811.12907)

Event	$m_1/M_\odot$	$m_2/M_\odot$	$\mathcal{M}/M_\odot$	$\chi_{\text{eff}}$	$M_f/M_\odot$	$a_f$	$E_{\text{rad}}/(M_\odot c^2)$	$\ell_{\text{peak}}/(\text{erg s}^{-1})$	$D_L/\text{Mpc}$	$z$	$\Delta\Omega/\text{deg}^2$
GW150914	$35.6^{+4.8}_{-3.0}$	$30.6^{+3.0}_{-4.4}$	$28.6^{+1.6}_{-1.5}$	$-0.01^{+0.12}_{-0.13}$	$63.1^{+3.3}_{-3.0}$	$0.69^{+0.05}_{-0.04}$	$3.1^{+0.4}_{-0.4}$	$3.6^{+0.4}_{-0.4} \times 10^{56}$	$430^{+150}_{-170}$	$0.09^{+0.03}_{-0.03}$	194
GW151012	$23.2^{+14.0}_{-5.4}$	$13.6^{+4.1}_{-4.8}$	$15.2^{+2.0}_{-1.2}$	$0.04^{+0.28}_{-0.19}$	$35.7^{+9.9}_{-3.7}$	$0.67^{+0.13}_{-0.11}$	$1.5^{+0.5}_{-0.5}$	$3.2^{+0.8}_{-1.7} \times 10^{56}$	$1060^{+540}_{-480}$	$0.21^{+0.09}_{-0.09}$	1491
GW151226	$13.7^{+8.8}_{-3.2}$	$7.7^{+2.2}_{-2.6}$	$8.9^{+0.3}_{-0.3}$	$0.18^{+0.20}_{-0.12}$	$20.5^{+6.4}_{-1.5}$	$0.74^{+0.07}_{-0.05}$	$1.0^{+0.1}_{-0.2}$	$3.4^{+0.7}_{-1.7} \times 10^{56}$	$440^{+180}_{-190}$	$0.09^{+0.04}_{-0.04}$	1075
GW170104	$31.0^{+7.2}_{-5.6}$	$20.1^{+4.9}_{-4.5}$	$21.5^{+2.1}_{-1.7}$	$-0.04^{+0.17}_{-0.20}$	$49.4^{+5.2}_{-3.9}$	$0.66^{+0.09}_{-0.11}$	$2.2^{+0.5}_{-0.5}$	$3.2^{+0.7}_{-1.0} \times 10^{56}$	$960^{+430}_{-410}$	$0.19^{+0.07}_{-0.08}$	912
GW170608	$11.2^{+5.4}_{-1.9}$	$7.5^{+1.5}_{-2.1}$	$7.9^{+0.2}_{-0.2}$	$0.04^{+0.19}_{-0.06}$	$17.9^{+3.4}_{-0.7}$	$0.69^{+0.04}_{-0.04}$	$0.8^{+0.1}_{-0.1}$	$3.4^{+0.5}_{-1.3} \times 10^{56}$	$320^{+120}_{-110}$	$0.07^{+0.02}_{-0.02}$	524
GW170729	$50.7^{+16.3}_{-10.2}$	$34.4^{+8.9}_{-10.2}$	$35.8^{+6.3}_{-4.9}$	$0.37^{+0.21}_{-0.26}$	$80.3^{+14.5}_{-10.3}$	$0.81^{+0.07}_{-0.13}$	$4.9^{+1.6}_{-1.7}$	$4.2^{+0.8}_{-1.5} \times 10^{56}$	$2760^{+1290}_{-1350}$	$0.48^{+0.18}_{-0.21}$	1069
GW170809	$35.2^{+8.3}_{-5.9}$	$23.8^{+5.2}_{-5.1}$	$25.0^{+2.1}_{-1.6}$	$0.07^{+0.17}_{-0.16}$	$56.4^{+5.2}_{-3.7}$	$0.70^{+0.08}_{-0.09}$	$2.7^{+0.6}_{-0.6}$	$3.5^{+0.6}_{-0.9} \times 10^{56}$	$990^{+320}_{-380}$	$0.20^{+0.05}_{-0.07}$	310
GW170814	$30.7^{+5.5}_{-2.9}$	$25.6^{+2.8}_{-4.0}$	$24.3^{+1.4}_{-1.1}$	$0.07^{+0.12}_{-0.11}$	$53.6^{+3.2}_{-2.5}$	$0.73^{+0.07}_{-0.05}$	$2.8^{+0.4}_{-0.3}$	$3.7^{+0.5}_{-0.5} \times 10^{56}$	$560^{+140}_{-210}$	$0.12^{+0.03}_{-0.04}$	99
GW170817	$1.46^{+0.12}_{-0.10}$	$1.27^{+0.09}_{-0.09}$	$1.186^{+0.001}_{-0.001}$	$0.00^{+0.02}_{-0.01}$	$\leq 2.8$	$\leq 0.89$	$\geq 0.04$	$\geq 0.1 \times 10^{56}$	$40^{+10}_{-10}$	$0.01^{+0.00}_{-0.00}$	22
GW170818	$35.5^{+7.5}_{-4.7}$	$26.9^{+4.4}_{-5.2}$	$26.7^{+2.1}_{-1.7}$	$-0.09^{+0.18}_{-0.21}$	$59.8^{+4.8}_{-3.7}$	$0.67^{+0.07}_{-0.08}$	$2.7^{+0.5}_{-0.5}$	$3.4^{+0.5}_{-0.7} \times 10^{56}$	$1020^{+430}_{-370}$	$0.20^{+0.07}_{-0.07}$	35
GW170823	$39.5^{+10.1}_{-6.6}$	$29.4^{+6.5}_{-7.1}$	$29.3^{+4.2}_{-3.1}$	$0.08^{+0.19}_{-0.22}$	$65.6^{+9.3}_{-6.5}$	$0.71^{+0.08}_{-0.09}$	$3.3^{+0.9}_{-0.8}$	$3.6^{+0.6}_{-0.9} \times 10^{56}$	$1860^{+840}_{-840}$	$0.34^{+0.13}_{-0.14}$	1780



# Table of O1 and O2 triggers with source properties

See [arXiv:1811.12907](https://arxiv.org/abs/1811.12907)

Virgo data contributed to Parameter Estimation of 5 events

Event	$m_1/M_\odot$	$m_2/M_\odot$	$\mathcal{M}/M_\odot$	$\chi_{\text{eff}}$	$M_f/M_\odot$	$a_f$	$E_{\text{rad}}/(M_\odot c^2)$	$\ell_{\text{peak}}/(\text{erg s}^{-1})$	$D_L/\text{Mpc}$	$z$	$\Delta\Omega/\text{deg}^2$
GW150914	$35.6^{+4.8}_{-3.0}$	$30.6^{+3.0}_{-4.4}$	$28.6^{+1.6}_{-1.5}$	$-0.01^{+0.12}_{-0.13}$	$63.1^{+3.3}_{-3.0}$	$0.69^{+0.05}_{-0.04}$	$3.1^{+0.4}_{-0.4}$	$3.6^{+0.4}_{-0.4} \times 10^{56}$	$430^{+150}_{-170}$	$0.09^{+0.03}_{-0.03}$	194
GW151012	$23.2^{+14.0}_{-5.4}$	$13.6^{+4.1}_{-4.8}$	$15.2^{+2.0}_{-1.2}$	$0.04^{+0.28}_{-0.19}$	$35.7^{+9.9}_{-3.7}$	$0.67^{+0.13}_{-0.11}$	$1.5^{+0.5}_{-0.5}$	$3.2^{+0.8}_{-1.7} \times 10^{56}$	$1060^{+540}_{-480}$	$0.21^{+0.09}_{-0.09}$	1491
GW151226	$13.7^{+8.8}_{-3.2}$	$7.7^{+2.2}_{-2.6}$	$8.9^{+0.3}_{-0.3}$	$0.18^{+0.20}_{-0.12}$	$20.5^{+6.4}_{-1.5}$	$0.74^{+0.07}_{-0.05}$	$1.0^{+0.1}_{-0.2}$	$3.4^{+0.7}_{-1.7} \times 10^{56}$	$440^{+180}_{-190}$	$0.09^{+0.04}_{-0.04}$	1075
GW170104	$31.0^{+7.2}_{-5.6}$	$20.1^{+4.9}_{-4.5}$	$21.5^{+2.1}_{-1.7}$	$-0.04^{+0.17}_{-0.20}$	$49.4^{+5.2}_{-3.9}$	$0.66^{+0.09}_{-0.11}$	$2.2^{+0.5}_{-0.5}$	$3.2^{+0.7}_{-1.0} \times 10^{56}$	$960^{+430}_{-410}$	$0.19^{+0.07}_{-0.08}$	912
GW170608	$11.2^{+5.4}_{-1.9}$	$7.5^{+1.5}_{-2.1}$	$7.9^{+0.2}_{-0.2}$	$0.04^{+0.19}_{-0.06}$	$17.9^{+3.4}_{-0.7}$	$0.69^{+0.04}_{-0.04}$	$0.8^{+0.1}_{-0.1}$	$3.4^{+0.5}_{-1.3} \times 10^{56}$	$320^{+120}_{-110}$	$0.07^{+0.02}_{-0.02}$	524
GW170729	$50.7^{+16.3}_{-10.2}$	$34.4^{+8.9}_{-10.2}$	$35.8^{+6.3}_{-4.9}$	$0.37^{+0.21}_{-0.26}$	$80.3^{+14.5}_{-10.3}$	$0.81^{+0.07}_{-0.13}$	$4.9^{+1.6}_{-1.7}$	$4.2^{+0.8}_{-1.5} \times 10^{56}$	$2760^{+1290}_{-1350}$	$0.48^{+0.18}_{-0.21}$	1069
GW170809	$35.2^{+8.3}_{-5.9}$	$23.8^{+5.2}_{-5.1}$	$25.0^{+2.1}_{-1.6}$	$0.07^{+0.17}_{-0.16}$	$56.4^{+5.2}_{-3.7}$	$0.70^{+0.08}_{-0.09}$	$2.7^{+0.6}_{-0.6}$	$3.5^{+0.6}_{-0.9} \times 10^{56}$	$990^{+320}_{-380}$	$0.20^{+0.05}_{-0.07}$	310
GW170814	$30.7^{+5.5}_{-2.9}$	$25.6^{+2.8}_{-4.0}$	$24.3^{+1.4}_{-1.1}$	$0.07^{+0.12}_{-0.11}$	$53.6^{+3.2}_{-2.5}$	$0.73^{+0.07}_{-0.05}$	$2.8^{+0.4}_{-0.3}$	$3.7^{+0.5}_{-0.5} \times 10^{56}$	$560^{+140}_{-210}$	$0.12^{+0.03}_{-0.04}$	99
GW170817	$1.46^{+0.12}_{-0.10}$	$1.27^{+0.09}_{-0.09}$	$1.186^{+0.001}_{-0.001}$	$0.00^{+0.02}_{-0.01}$	$\leq 2.8$	$\leq 0.89$	$\geq 0.04$	$\geq 0.1 \times 10^{56}$	$40^{+10}_{-10}$	$0.01^{+0.00}_{-0.00}$	22
GW170818	$35.5^{+7.5}_{-4.7}$	$26.9^{+4.4}_{-5.2}$	$26.7^{+2.1}_{-1.7}$	$-0.09^{+0.18}_{-0.21}$	$59.8^{+4.8}_{-3.7}$	$0.67^{+0.07}_{-0.08}$	$2.7^{+0.5}_{-0.5}$	$3.4^{+0.5}_{-0.7} \times 10^{56}$	$1020^{+430}_{-370}$	$0.20^{+0.07}_{-0.07}$	35
GW170823	$39.5^{+10.1}_{-6.6}$	$29.4^{+6.5}_{-7.1}$	$29.3^{+4.2}_{-3.1}$	$0.08^{+0.19}_{-0.22}$	$65.6^{+9.3}_{-6.5}$	$0.71^{+0.08}_{-0.09}$	$3.3^{+0.9}_{-0.8}$	$3.6^{+0.6}_{-0.9} \times 10^{56}$	$1860^{+840}_{-840}$	$0.34^{+0.13}_{-0.14}$	1780



# Table of O1 and O2 triggers with source properties

See [arXiv:1811.12907](https://arxiv.org/abs/1811.12907)

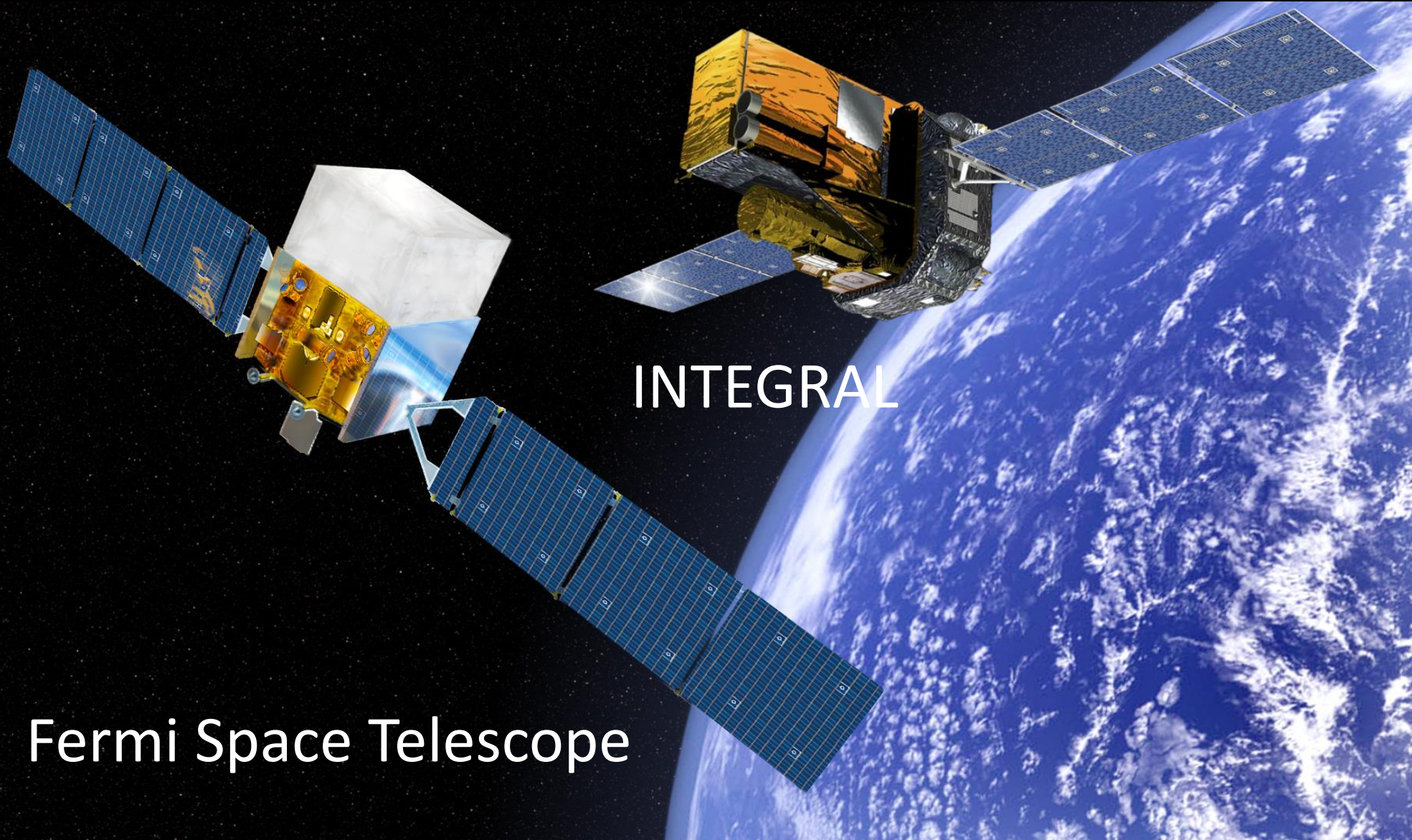
GW180817 is a binary neutron star merger event. The others are black hole mergers

Event	$m_1/M_\odot$	$m_2/M_\odot$	$\mathcal{M}/M_\odot$	$\chi_{\text{eff}}$	$M_f/M_\odot$	$a_f$	$E_{\text{rad}}/(M_\odot c^2)$	$\ell_{\text{peak}}/(\text{erg s}^{-1})$	$D_L/\text{Mpc}$	$z$	$\Delta\Omega/\text{deg}^2$
GW150914	$35.6^{+4.8}_{-3.0}$	$30.6^{+3.0}_{-4.4}$	$28.6^{+1.6}_{-1.5}$	$-0.01^{+0.12}_{-0.13}$	$63.1^{+3.3}_{-3.0}$	$0.69^{+0.05}_{-0.04}$	$3.1^{+0.4}_{-0.4}$	$3.6^{+0.4}_{-0.4} \times 10^{56}$	$430^{+150}_{-170}$	$0.09^{+0.03}_{-0.03}$	194
GW151012	$23.2^{+14.0}_{-5.4}$	$13.6^{+4.1}_{-4.8}$	$15.2^{+2.0}_{-1.2}$	$0.04^{+0.28}_{-0.19}$	$35.7^{+9.9}_{-3.7}$	$0.67^{+0.13}_{-0.11}$	$1.5^{+0.5}_{-0.5}$	$3.2^{+0.8}_{-1.7} \times 10^{56}$	$1060^{+540}_{-480}$	$0.21^{+0.09}_{-0.09}$	1491
GW151226	$13.7^{+8.8}_{-3.2}$	$7.7^{+2.2}_{-2.6}$	$8.9^{+0.3}_{-0.3}$	$0.18^{+0.20}_{-0.12}$	$20.5^{+6.4}_{-1.5}$	$0.74^{+0.07}_{-0.05}$	$1.0^{+0.1}_{-0.2}$	$3.4^{+0.7}_{-1.7} \times 10^{56}$	$440^{+180}_{-190}$	$0.09^{+0.04}_{-0.04}$	1075
GW170104	$31.0^{+7.2}_{-5.6}$	$20.1^{+4.9}_{-4.5}$	$21.5^{+2.1}_{-1.7}$	$-0.04^{+0.17}_{-0.20}$	$49.4^{+5.2}_{-3.9}$	$0.66^{+0.09}_{-0.11}$	$2.2^{+0.5}_{-0.5}$	$3.2^{+0.7}_{-1.0} \times 10^{56}$	$960^{+430}_{-410}$	$0.19^{+0.07}_{-0.08}$	912
GW170608	$11.2^{+5.4}_{-1.9}$	$7.5^{+1.5}_{-2.1}$	$7.9^{+0.2}_{-0.2}$	$0.04^{+0.19}_{-0.06}$	$17.9^{+3.4}_{-0.7}$	$0.69^{+0.04}_{-0.04}$	$0.8^{+0.1}_{-0.1}$	$3.4^{+0.5}_{-1.3} \times 10^{56}$	$320^{+120}_{-110}$	$0.07^{+0.02}_{-0.02}$	524
GW170729	$50.7^{+16.3}_{-10.2}$	$34.4^{+8.9}_{-10.2}$	$35.8^{+6.3}_{-4.9}$	$0.37^{+0.21}_{-0.26}$	$80.3^{+14.5}_{-10.3}$	$0.81^{+0.07}_{-0.13}$	$4.9^{+1.6}_{-1.7}$	$4.2^{+0.8}_{-1.5} \times 10^{56}$	$2760^{+1290}_{-1350}$	$0.48^{+0.18}_{-0.21}$	1069
GW170809	$35.2^{+8.3}_{-5.9}$	$23.8^{+5.2}_{-5.1}$	$25.0^{+2.1}_{-1.6}$	$0.07^{+0.17}_{-0.16}$	$56.4^{+5.2}_{-3.7}$	$0.70^{+0.08}_{-0.09}$	$2.7^{+0.6}_{-0.6}$	$3.5^{+0.6}_{-0.9} \times 10^{56}$	$990^{+320}_{-380}$	$0.20^{+0.05}_{-0.07}$	310
GW170814	$30.7^{+5.5}_{-2.9}$	$25.6^{+2.8}_{-4.0}$	$24.3^{+1.4}_{-1.1}$	$0.07^{+0.12}_{-0.11}$	$53.6^{+3.2}_{-2.5}$	$0.73^{+0.07}_{-0.05}$	$2.8^{+0.4}_{-0.3}$	$3.7^{+0.5}_{-0.5} \times 10^{56}$	$560^{+140}_{-210}$	$0.12^{+0.03}_{-0.04}$	99
GW170817	$1.46^{+0.12}_{-0.10}$	$1.27^{+0.09}_{-0.09}$	$1.186^{+0.001}_{-0.001}$	$0.00^{+0.02}_{-0.01}$	$\leq 2.8$	$\leq 0.89$	$\geq 0.04$	$\geq 0.1 \times 10^{56}$	$40^{+10}_{-10}$	$0.01^{+0.00}_{-0.00}$	22
GW170818	$35.5^{+7.5}_{-4.7}$	$26.9^{+4.4}_{-5.2}$	$26.7^{+2.1}_{-1.7}$	$-0.09^{+0.18}_{-0.21}$	$59.8^{+4.8}_{-3.7}$	$0.67^{+0.07}_{-0.08}$	$2.7^{+0.5}_{-0.5}$	$3.4^{+0.5}_{-0.7} \times 10^{56}$	$1020^{+430}_{-370}$	$0.20^{+0.07}_{-0.07}$	35
GW170823	$39.5^{+10.1}_{-6.6}$	$29.4^{+6.5}_{-7.1}$	$29.3^{+4.2}_{-3.1}$	$0.08^{+0.19}_{-0.22}$	$65.6^{+9.3}_{-6.5}$	$0.71^{+0.08}_{-0.09}$	$3.3^{+0.9}_{-0.8}$	$3.6^{+0.6}_{-0.9} \times 10^{56}$	$1860^{+840}_{-840}$	$0.34^{+0.13}_{-0.14}$	1780



Some scientific highlights: neutron stars

Gamma rays reached Earth 1.7 seconds after GW180717

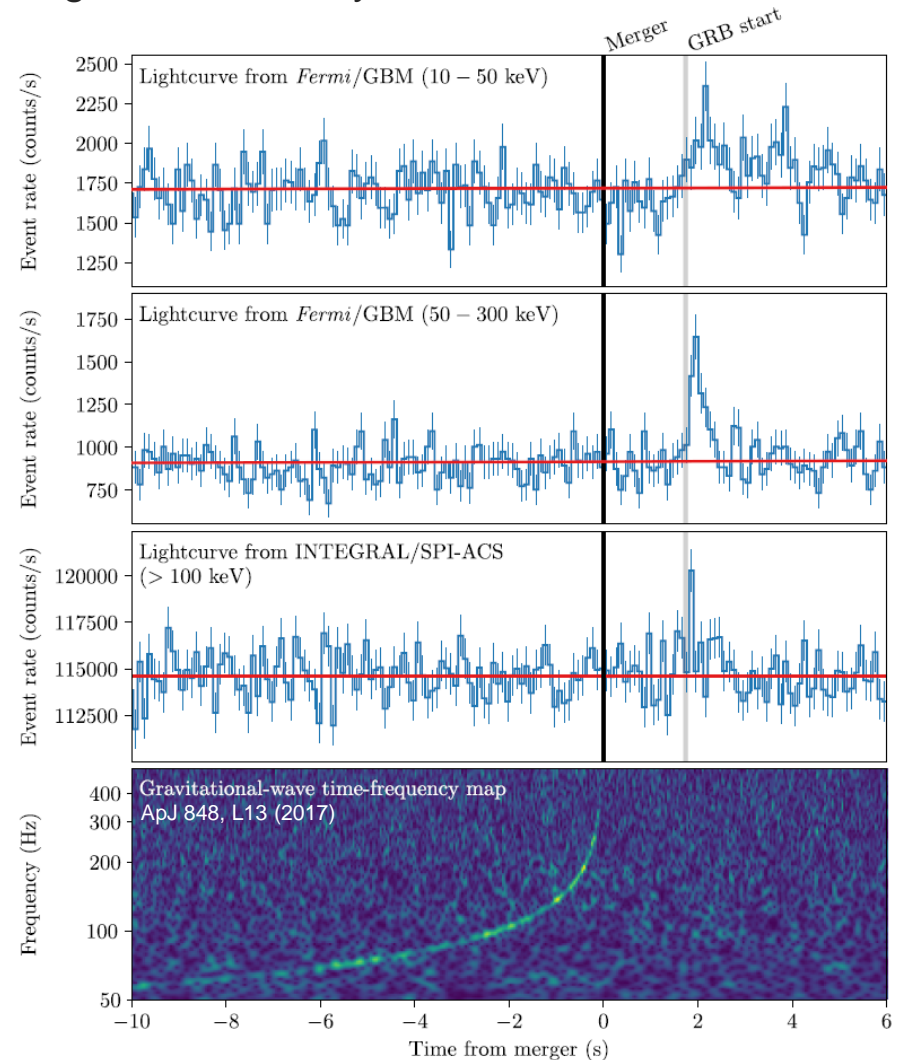


INTEGRAL

Fermi Space Telescope

# Binary neutron star merger on August 17, 2017

Gamma rays reached Earth 1.7 s after the end of the gravitational wave inspiral signal. The data are consistent with standard EM theory minimally coupled to general relativity



## Neutron stars are laboratories for extreme physics

Mass: from about 1.1 to about 2.2 solar mass

Density: up to several times nuclear density

Temperature: up to  $10^{12}$  K

Magnetic field: up to  $10^{11}$  T

Held together by gravity and supported by degeneracy pressure and NN repulsion

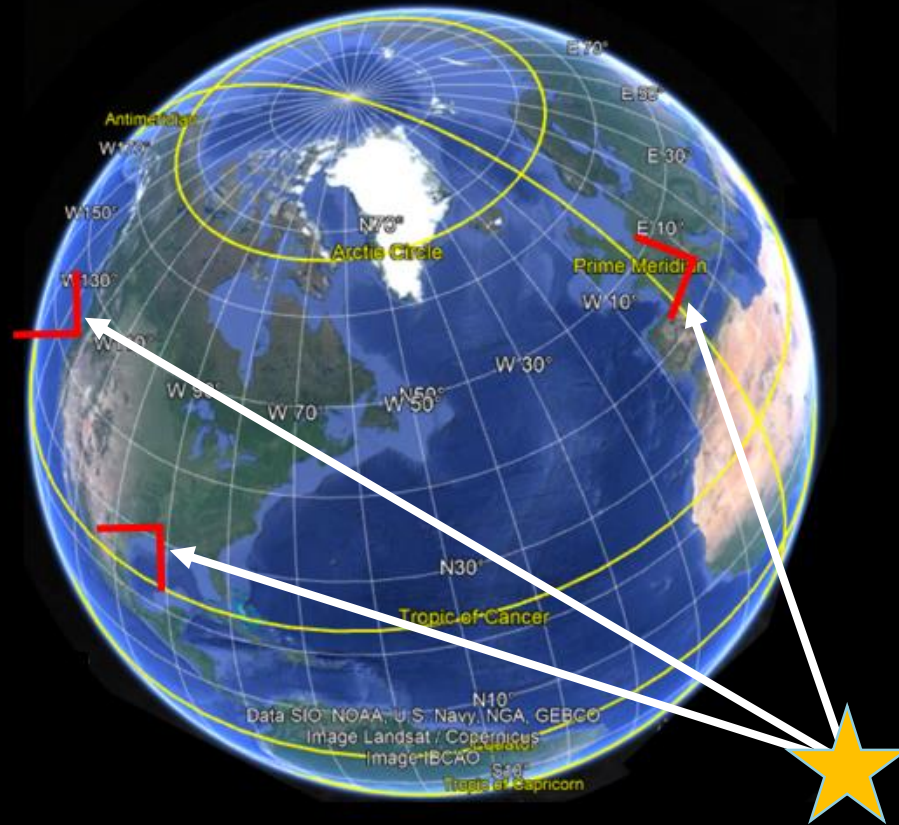
Extrapolate behavior of QCD, superconductivity, and superfluidity

Equation Of State: many models

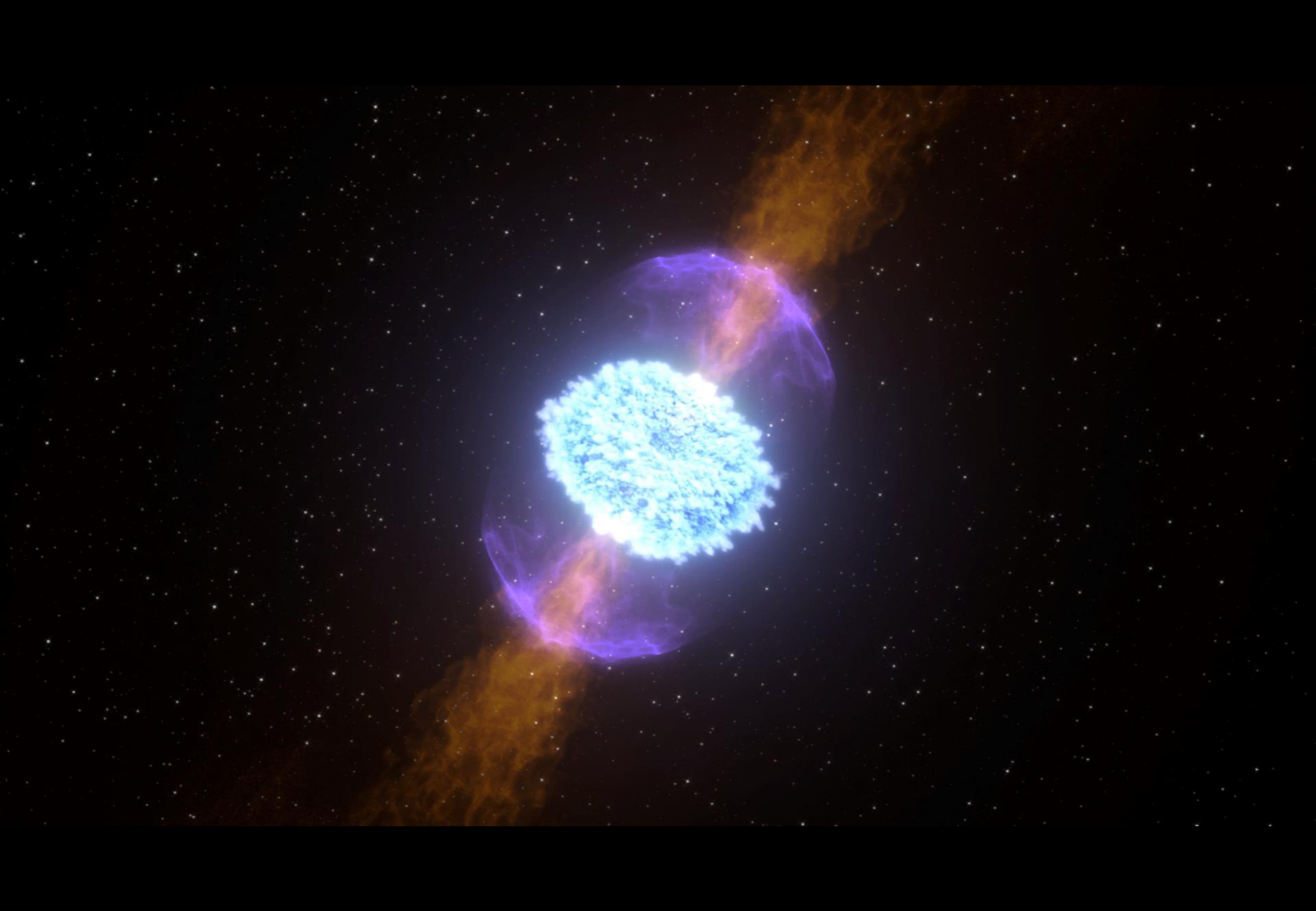


# Source location via triangulation

GW170817 first arrived at Virgo, after 22 ms it arrived at LLO, and another 3 ms later LLH detected it







# Implications for fundamental physics

Gamma rays reached Earth 1.7 s after the end of the gravitational wave inspiral signal. The data are consistent with standard EM theory minimally coupled to general relativity

## GWs and light propagation speeds

Identical speeds to (assuming conservative lower bound on distance from GW signal of 26 Mpc)

$$-3 \times 10^{-15} < \frac{\Delta v}{v_{EM}} < +7 \times 10^{-16}$$

## Test of Equivalence Principle

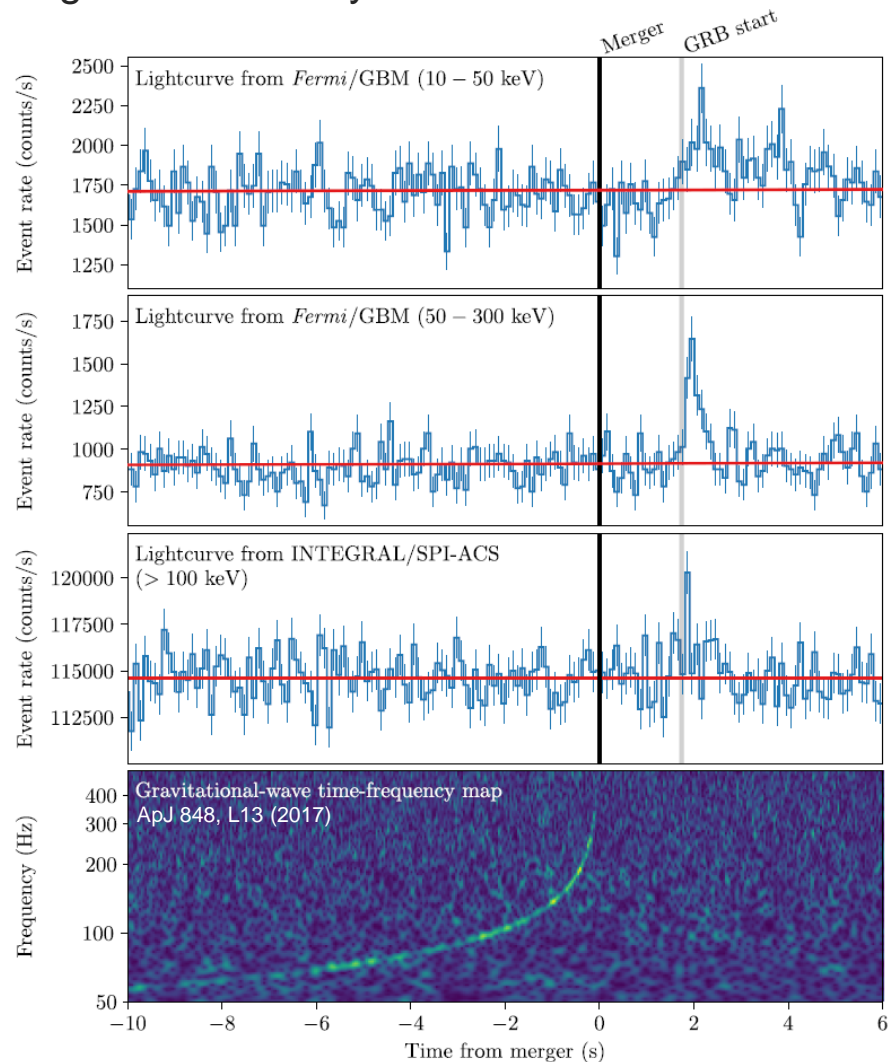
According to General Relativity, GW and EM waves are deflected and delayed by the curvature of spacetime produced by any mass (i.e. background gravitational potential). Shapiro delays affect both waves in the same manner

$$\Delta t_{\text{gravity}} = -\frac{\Delta\gamma}{c^3} \int_{r_0}^{r_e} U(r(t); t) dr$$

Milky Way potential gives same effect to within

$$-2.6 \times 10^{-7} \leq \gamma_{\text{GW}} - \gamma_{\text{EM}} \leq 1.2 \times 10^{-6}$$

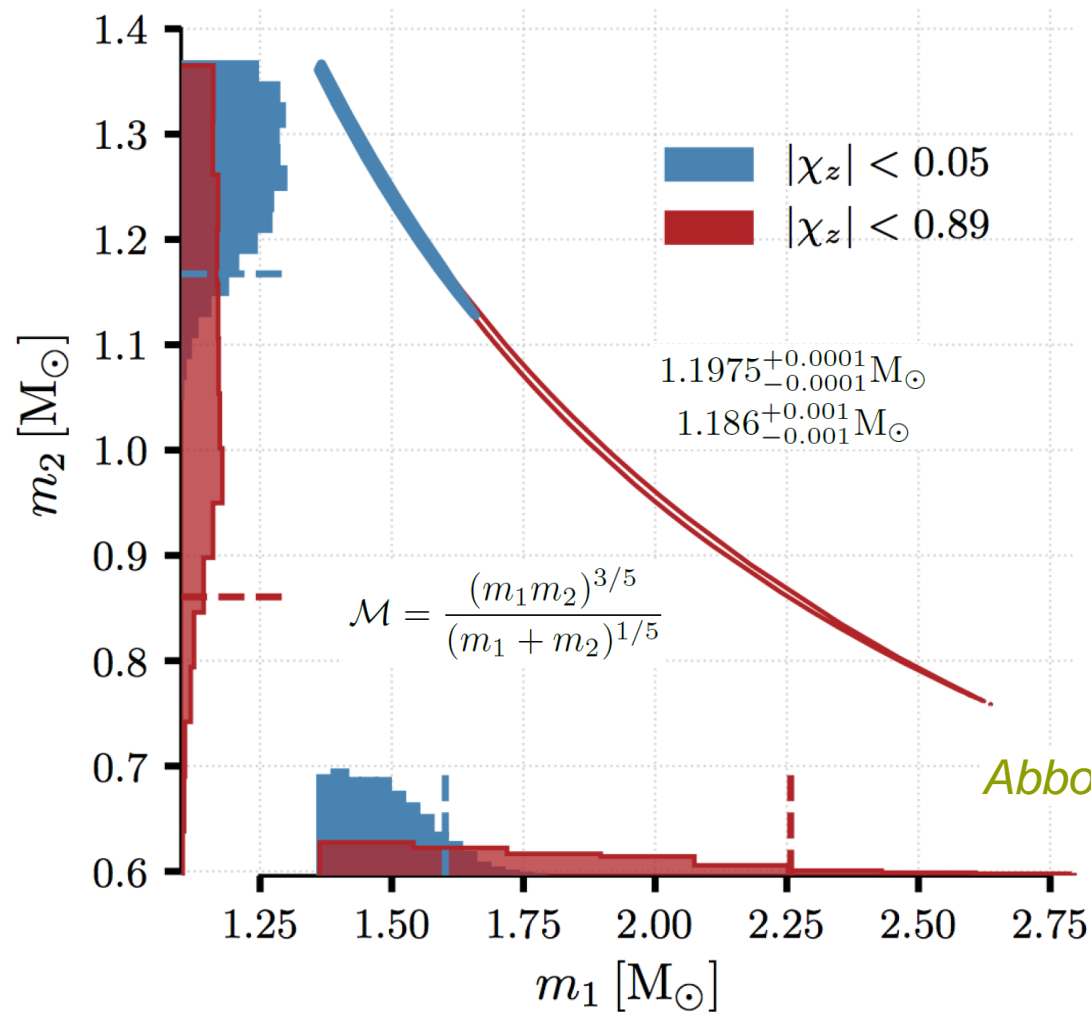
Including data on peculiar velocities to 50 Mpc we find  $\Delta\gamma \leq 4 \times 10^{-9}$



# Inferring neutron star properties: masses

Early estimates now improved using known source location, improved waveform modeling, and re-calibrated Virgo data. Chirp mass can be inferred to high precision. There is a degeneracy between masses and spins

Observation of **binary pulsars** in our galaxy indicates spins are **not larger than ~0.04**



To lowest approximation  $\tilde{h}(f) \propto e^{i\Psi(f)}$

$$\text{with } \Psi(f) = \frac{3}{4} \left( \frac{G\mathcal{M}}{c^3} 8\pi f \right)^{-5/3} + \dots$$

*Abbott et al. PRL 119 (2017) 161101*

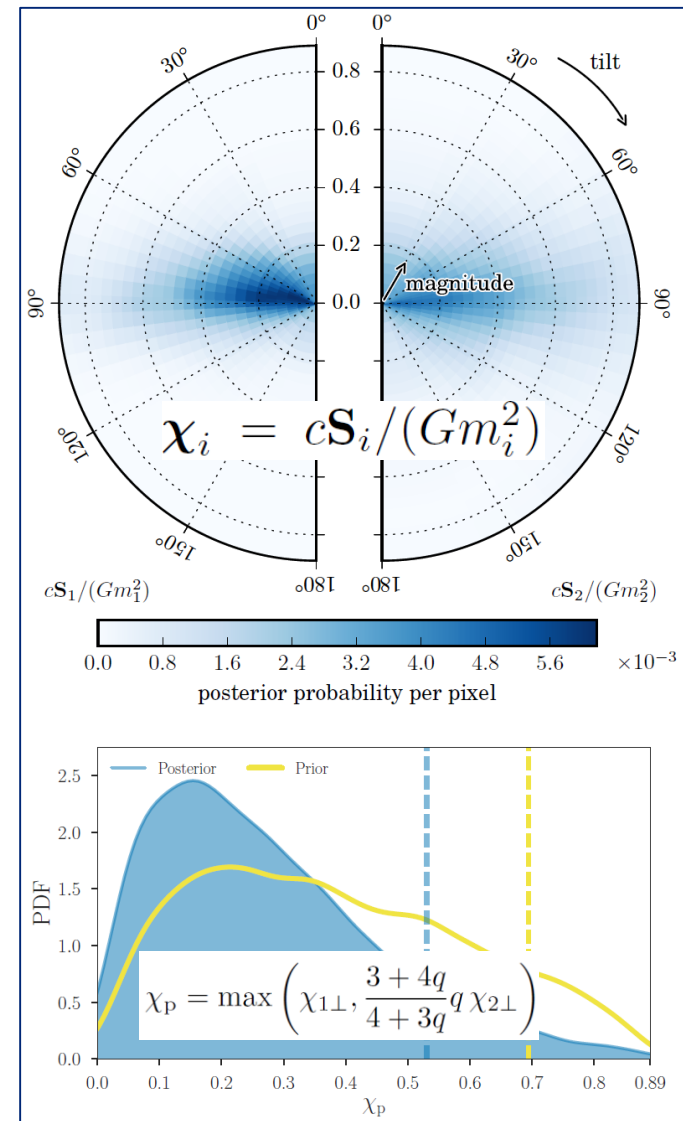
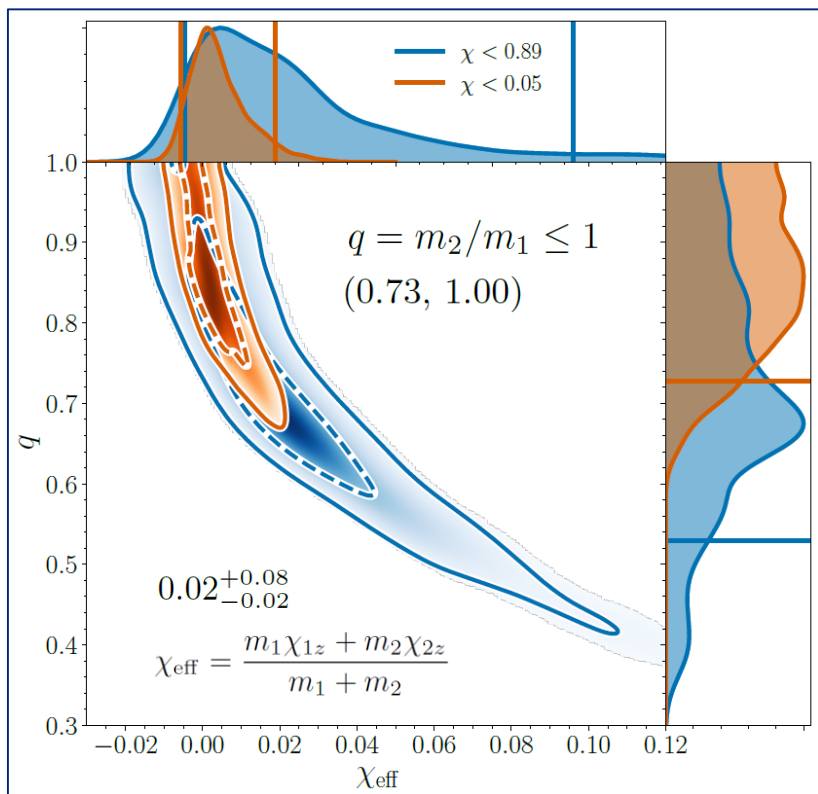
# Inferring neutron star properties: spins

Constrains on mass ratio  $q$ ,  $\chi_i$  dimensionless spin,  $\chi_{\text{eff}}$  effective spin, and  $\chi_p$  effective spin precession parameter. See <https://arxiv.org/abs/1805.11579>

No evidence for NS spin

$\chi_{\text{eff}}$  contributes to GW phase at 1.5 PN, and degenerate with  $q$

$\chi_p$  starts contributing at 2 PN

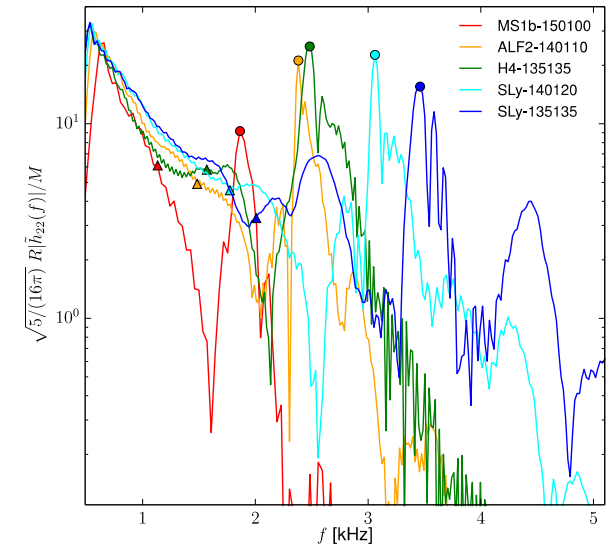
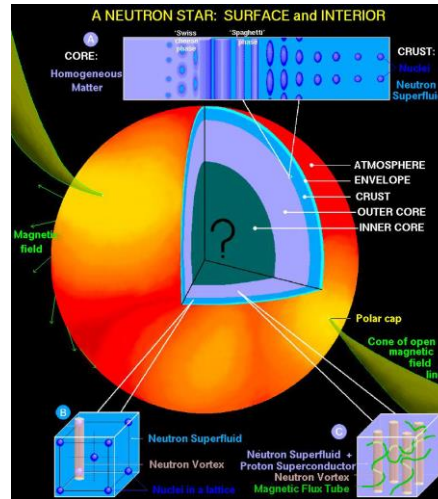


# Solving an astrophysical conundrum

Neutron stars are rich laboratories with extreme matter physics in a strong gravitational environment. Stability is obtained due to quantum physics

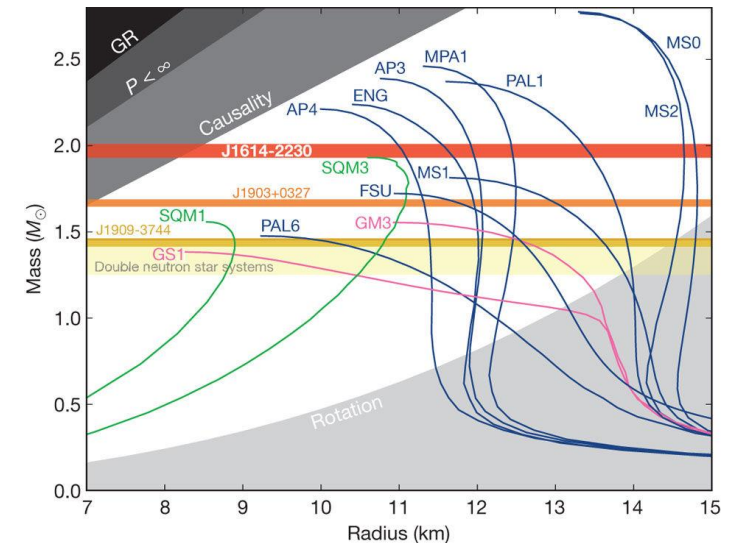
## Structure of neutron stars?

- Structure of the crust?
- Proton superconductivity
- Neutron superfluidity
- “Pinning” of fluid vortices to crust
- Origin of magnetic fields?
- More exotic objects?



## Widely differing theoretical predictions for different equations of state

- Pressure as a function of density
- Mass as a function of radius
- Tidal deformability as a function of mass
- Post-merger signal depends on EOS
  - “Soft”: prompt collapse to black hole
  - “Hard”: hypermassive neutron star



Demorest *et al.*, Nature 467, 1081 (2010)

Bernuzzi *et al.*, PRL 115, 091101 (2015)

# Probing the structure of neutron stars

Tidal effects leave their imprint on the gravitational wave signal from binary neutron stars. This provides information about their deformability. There is a strong need for more sensitive detectors

## Gravitational waves from inspiraling binary neutron stars

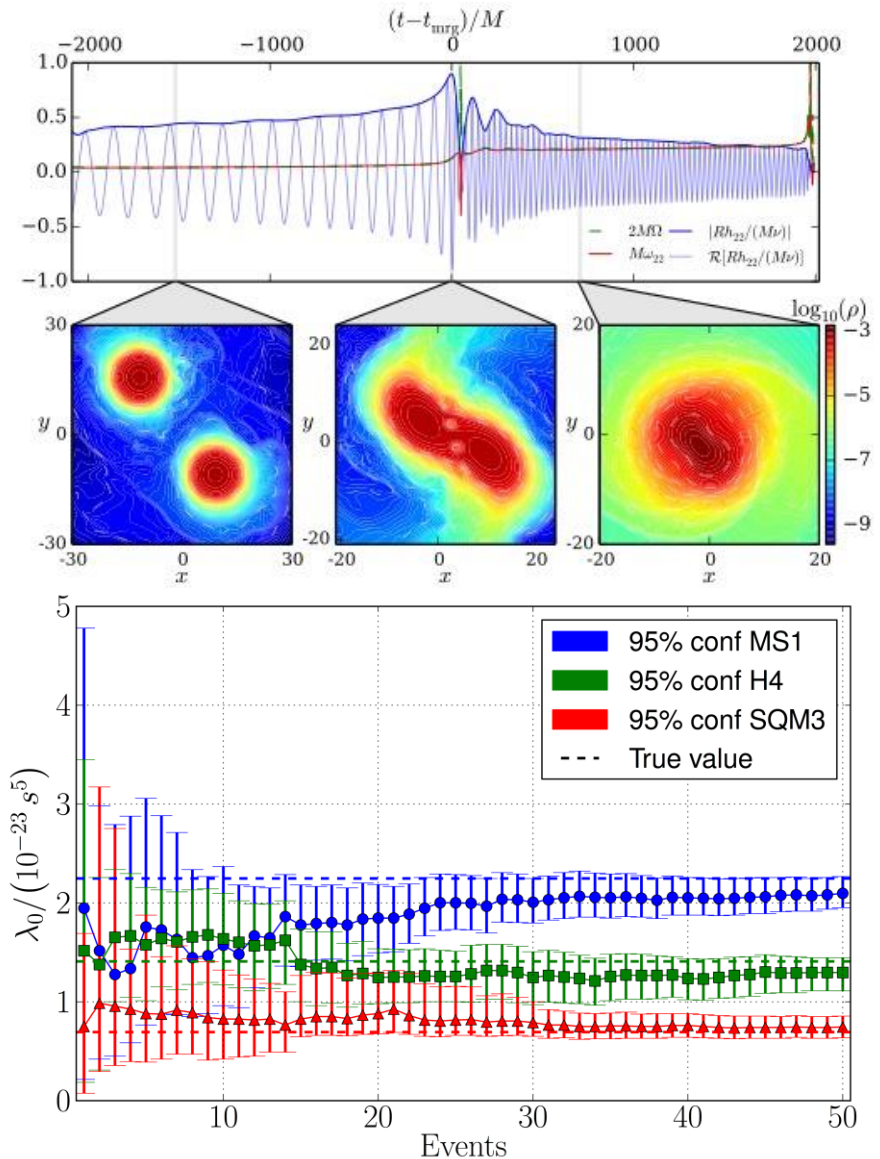
- When close, the stars induce tidal deformations in each other
- These affect orbital motion
- Tidal effects imprinted upon gravitational wave signal
- Tidal deformability maps directly to neutron star equation of state

## Measurement of tidal deformations on GW170817

- More compact neutron stars favored
- “Soft” equation of state

LIGO + Virgo, PRL 119, 161101 (2017)

Bernuzzi, Nagar, Font, ...

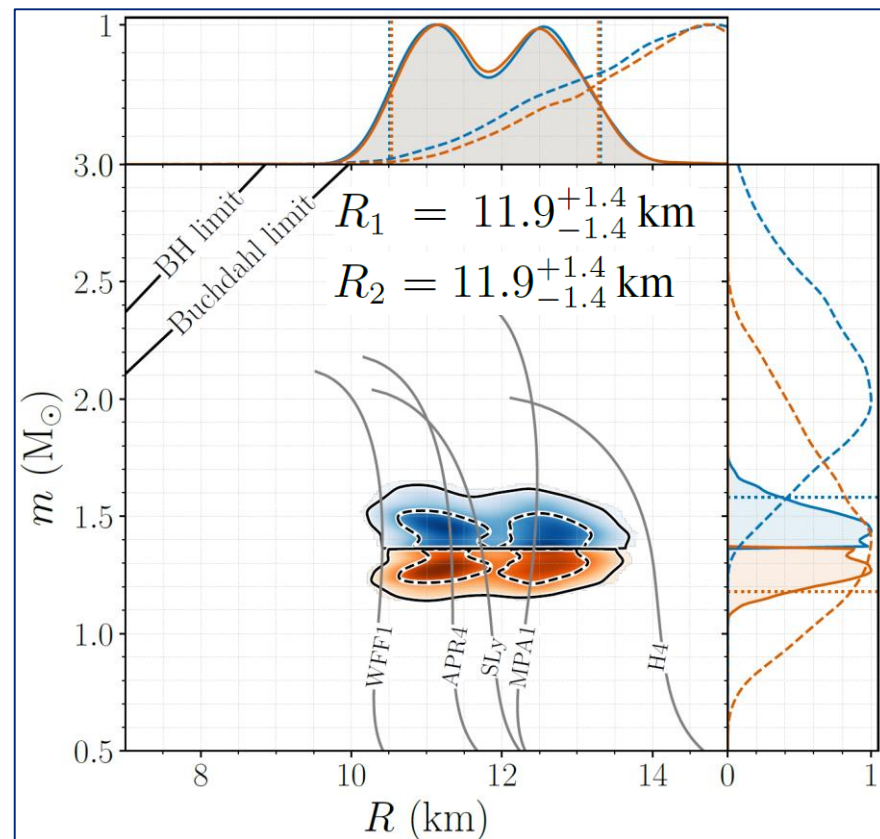
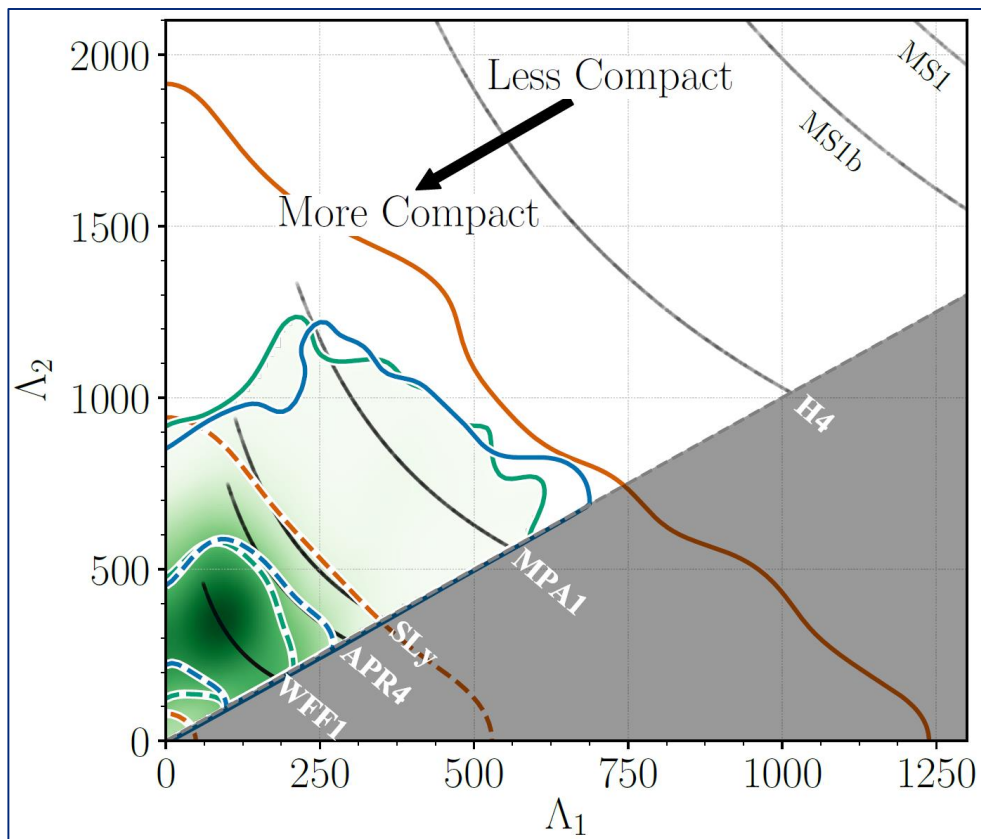


# Event GW170817: tidal deformability, EOS, radii

Tidal deformability gives support for “soft” EOS, leading to more compact NS. Various models can now be excluded. We can place the additional constraint that the EOS must support a NS  $1.97 M_{\odot}$

Leading tidal contribution to GW phase appears at 5 PN:  $\tilde{\Lambda} = \frac{16}{13} \frac{(m_1 + 12m_2)m_1^4\Lambda_1 + (m_2 + 12m_1)m_2^4\Lambda_2}{(m_1 + m_2)^5}$

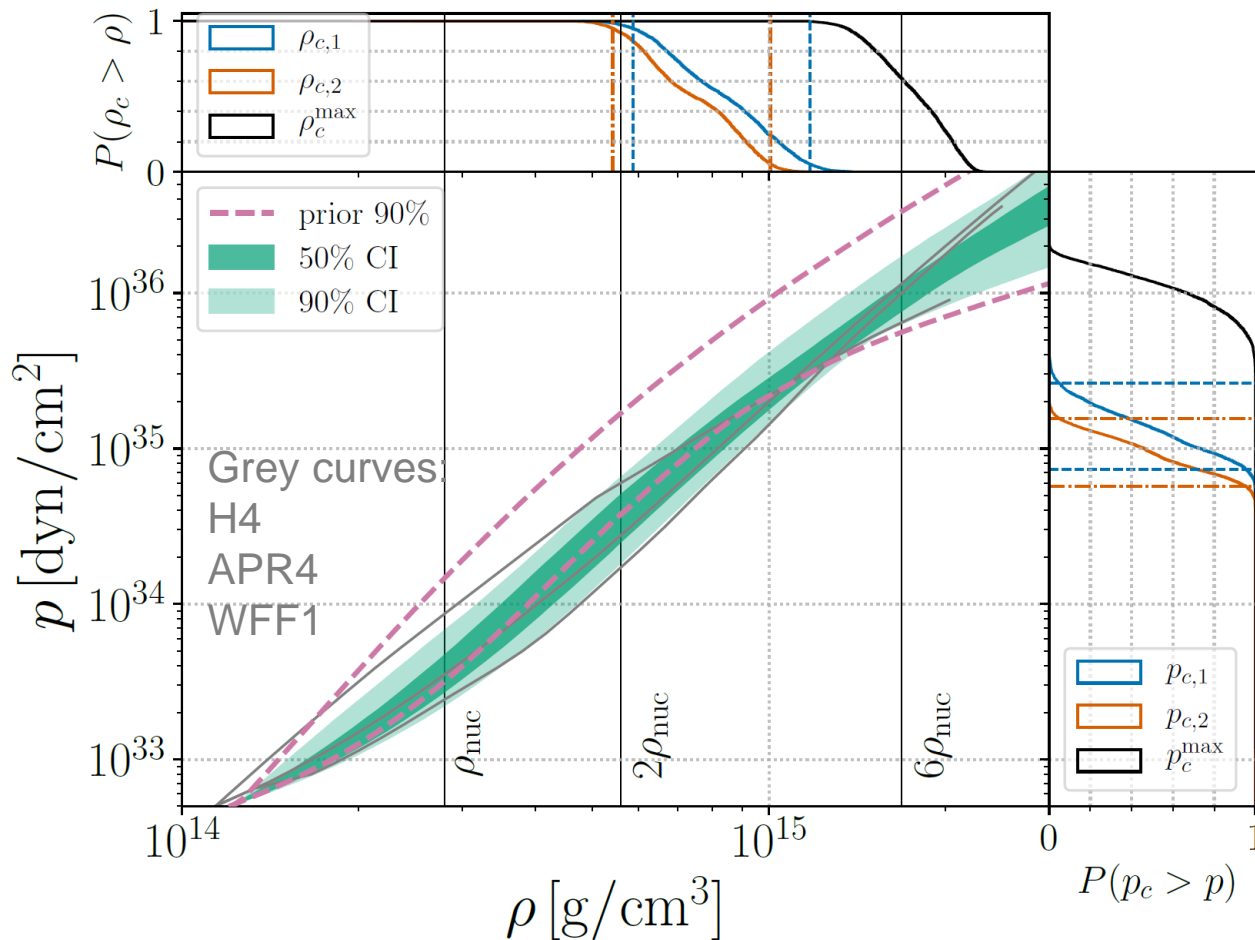
Employ common EOS for both NS (green shading), EOS insensitive relations (green), parametrized EOS (blue), independent EOSs (orange). See: LVC, <https://arxiv.org/abs/1805.11581>



# Pressure versus rest-mass density of NS interior

Spectral EOS parametrization and imposing a lower limit on the maximum NS mass supported by the EOS of  $1.97 M_{\text{solar}}$

The pressure posterior is shifted from the 90% credible prior region (marked by the purple dashed lines) and towards the soft floor of the parametrized family of EOS



No experimental support for new degrees of freedom or phase transition around five times nuclear density

See: LVC,  
<https://arxiv.org/abs/1805.11581>

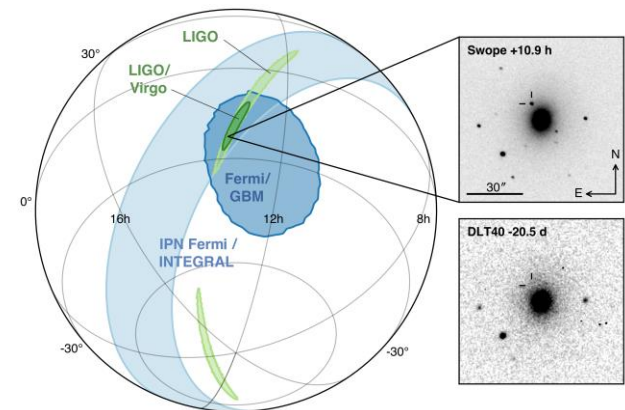
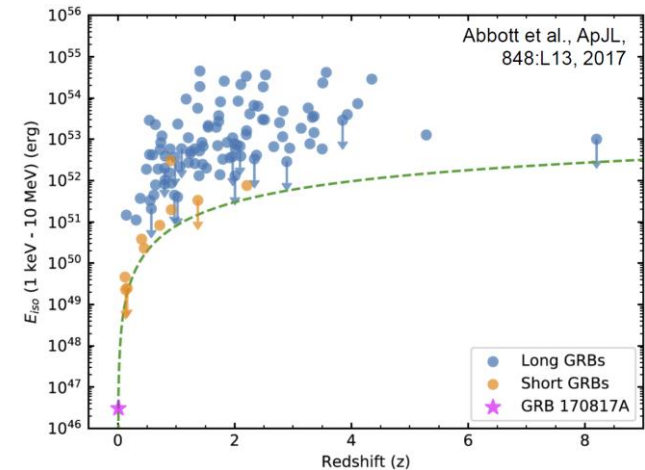
# Looking into the heart of a dim nearby sGRB

Gravitational waves identified the progenitor of the sGRB and provided both space localization and distance of the source. This triggered the EM follow-up by astronomers for the kilonova

Closest by and weakest sGRB, highest SNR GW event

LIGO/Virgo network allowed source localization of  $28 \text{ (degr)}^2$  and distance measurement of 40 Mpc

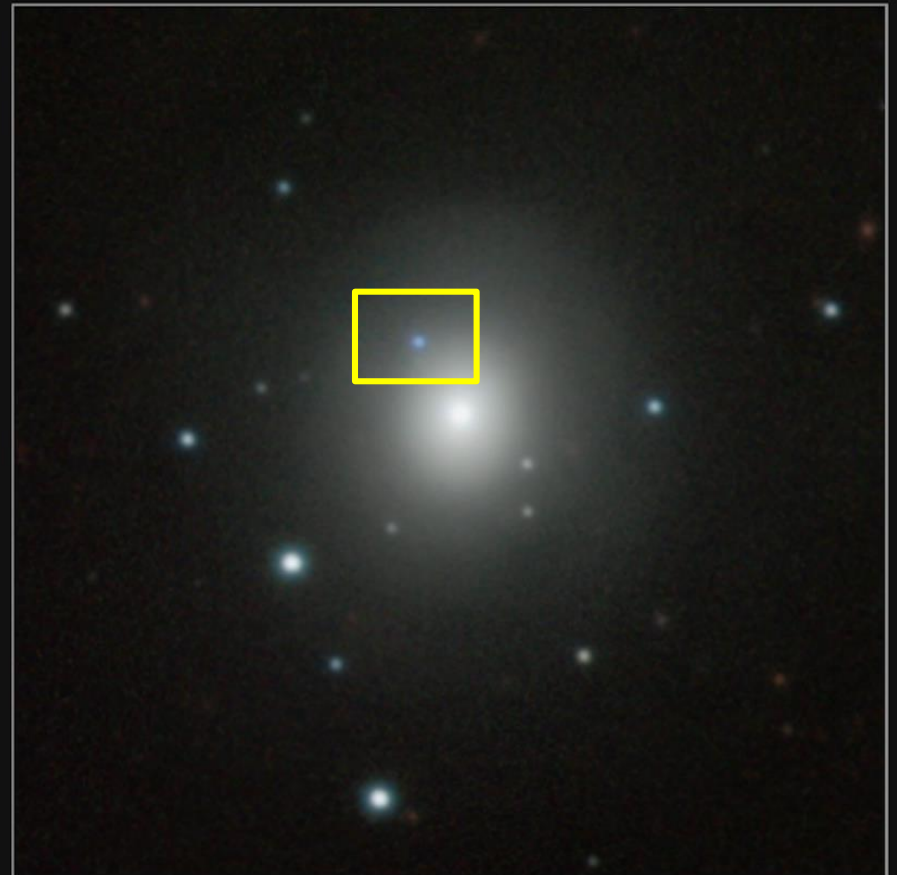
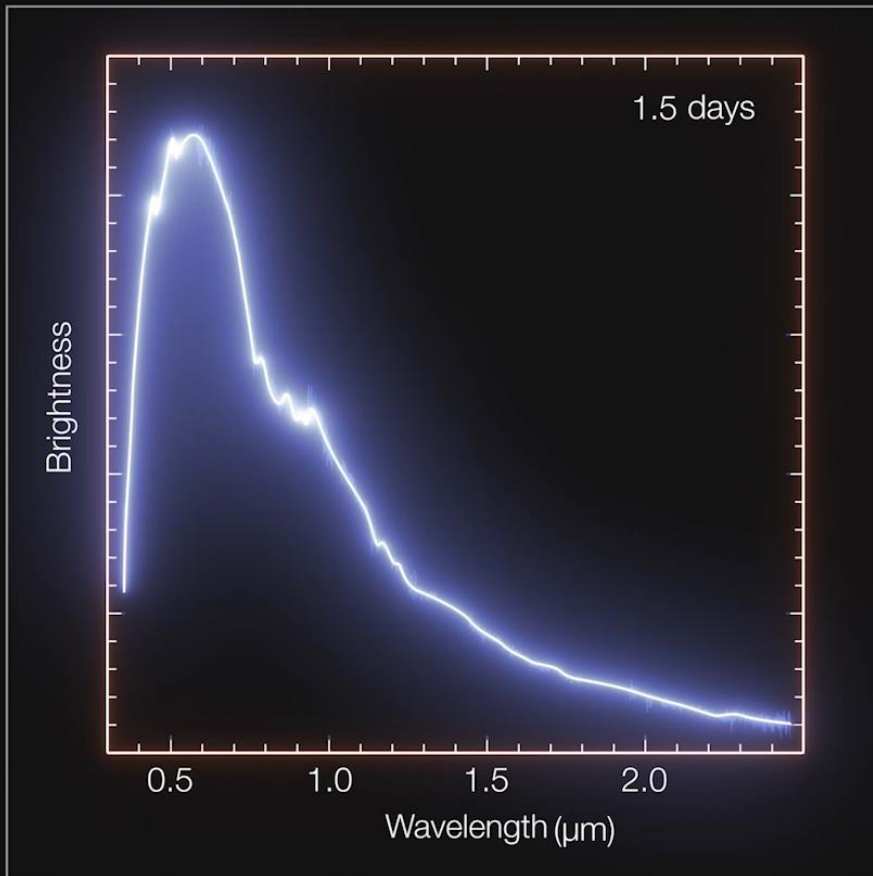
This allowed astronomers to study for the first time a kilonova, the r-process production of elements, a rapidly fading source



# European Southern Observatory

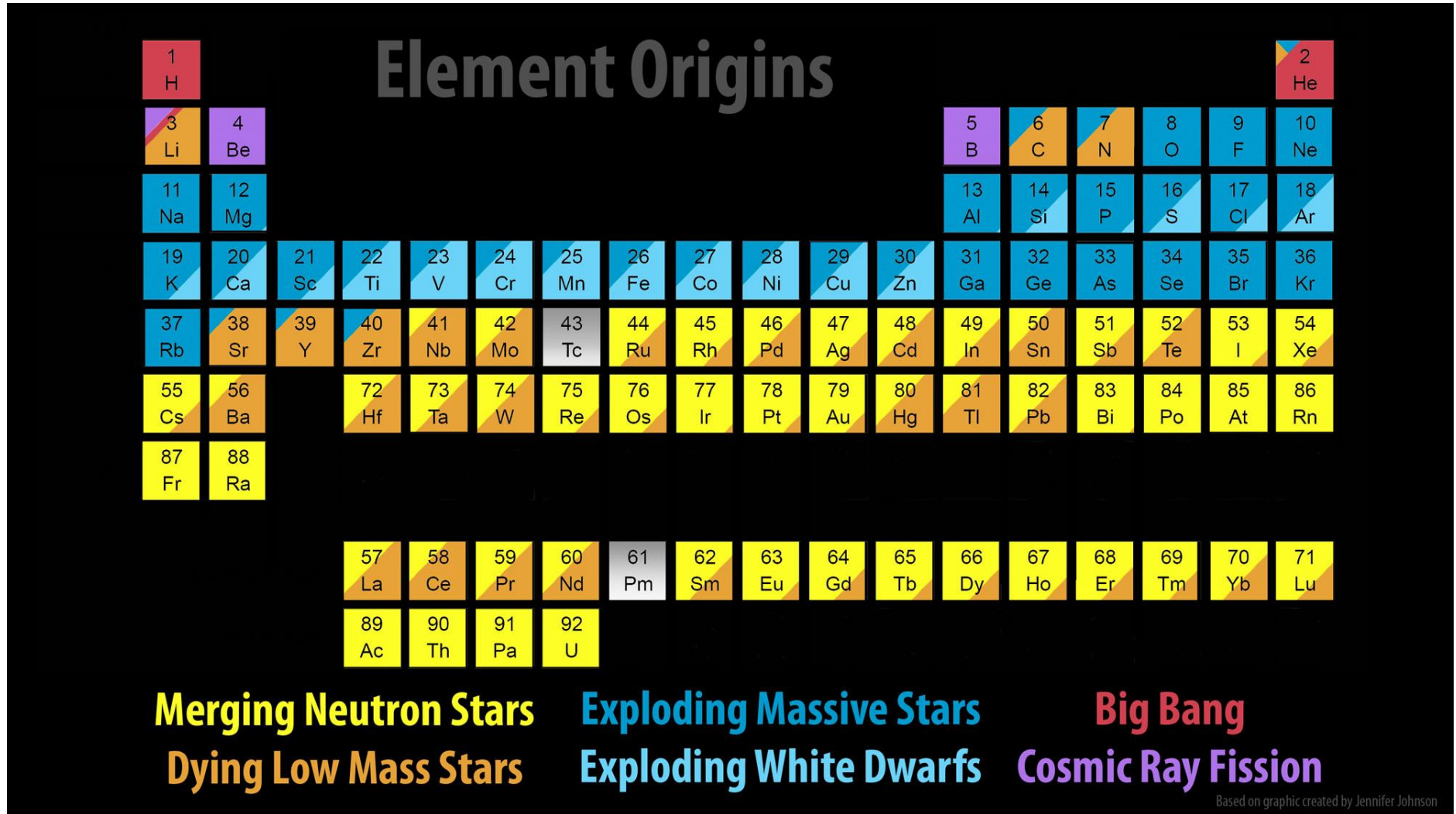
About 70 observatories worldwide observed the event by using space telescope (e.g. Hubble and Chandra) and ground-based telescopes (e.g. ESO) in all frequency bands (UVOIR). We witness the creation of heavy elements by studying their spectral evolution

Since LIGO/Virgo provide the distance and BNS source type, it was recognized that we are dealing with a weak (non-standard) GRB. This led to the optical counterpart to be found in this region



# Many heavy elements were produced in such collisions

GW170817 does not allow identification of spectra of these individual elements



# Identification of strontium in event GW170817

Identification of Strontium, an element that could only have been synthesised so quickly under an extreme neutron flux, provides the first direct spectroscopic evidence that neutron stars comprise neutron-rich matter

The kilonova essentially has a blackbody (blue dotted lines) with a temperature of 3,700 K

Assume solar r-process abundance ratios

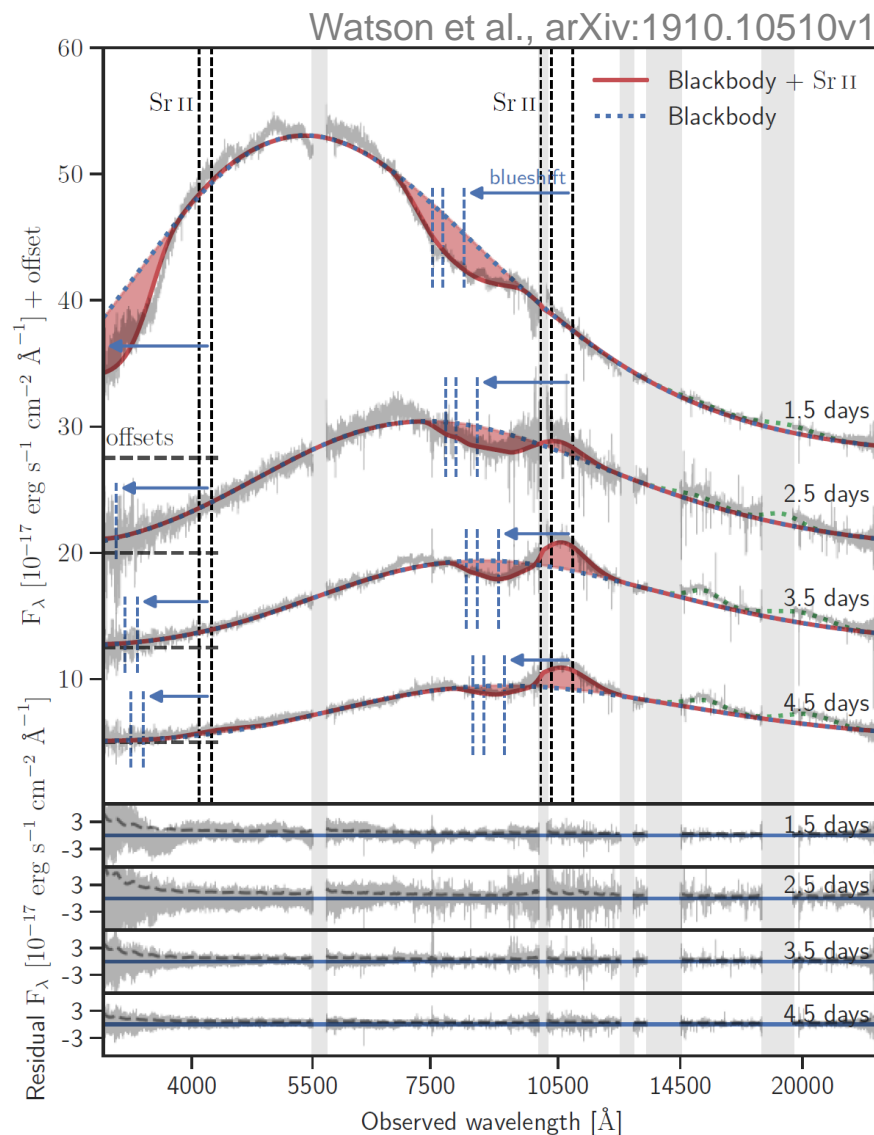
Sr accounts for at least a few percent by mass of all r-process elements

P Cygni profiles (red transparent fill) increasingly develop in time for the Sr lines

Lines are Doppler broadened by 0.2 c due to the high speed of the ejected material and blue-shifted by 0.23 c

Extreme-density stars composed of neutrons were proposed shortly after the discovery of the neutron, and identified with pulsars three decades later

GW170817 provides first spectroscopic evidence of neutron-rich matter in neutron stars

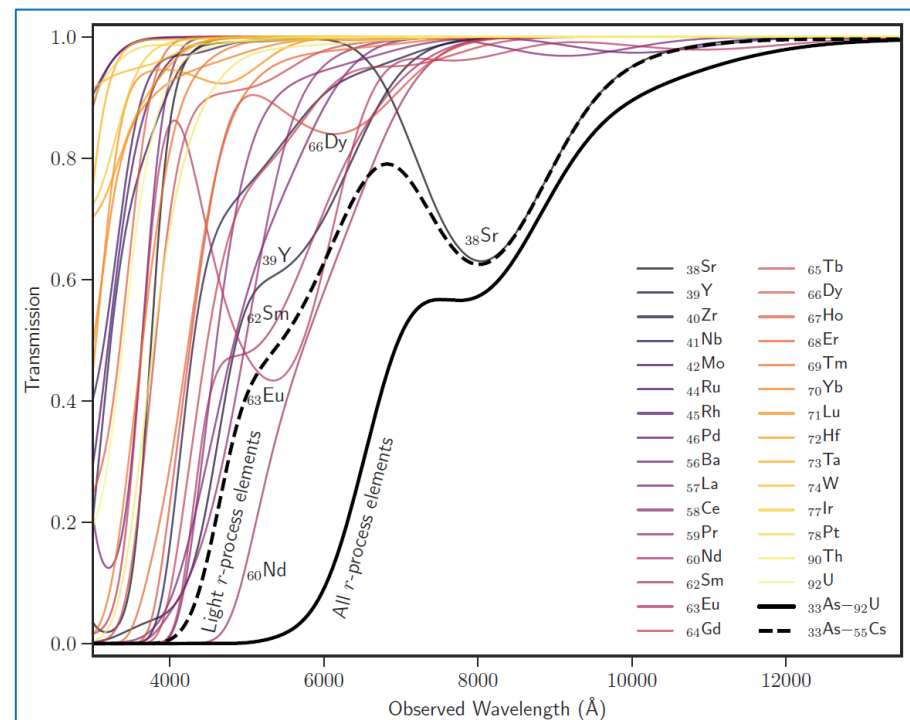
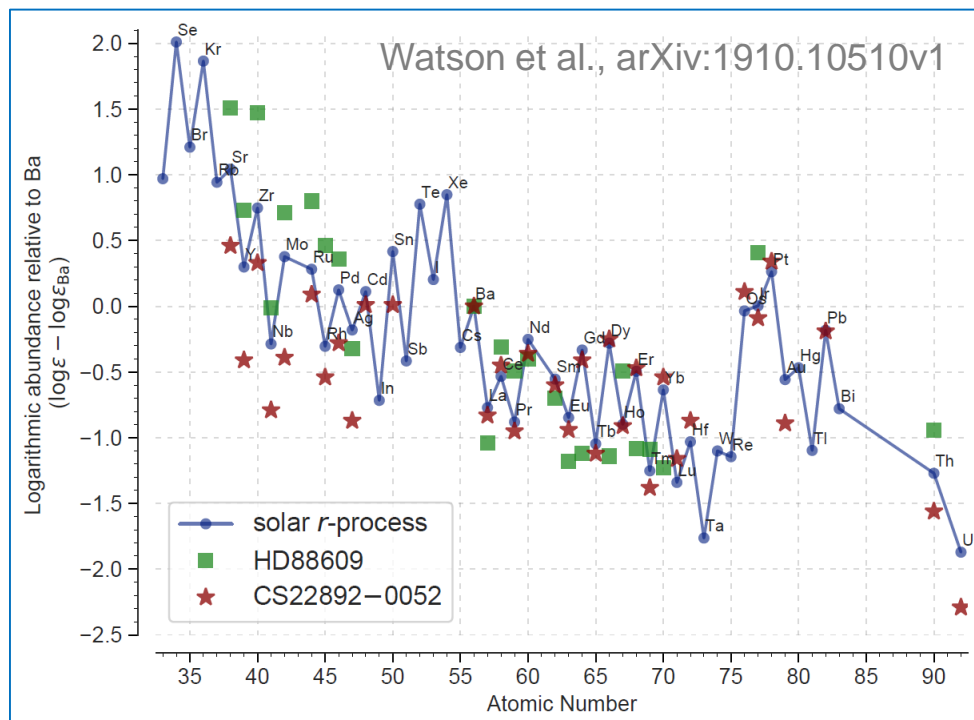


# Identification of strontium in event GW170817

Identification of Strontium through spectral modeling with a LTE spectral synthesis code, the LTE line analysis and spectrum synthesis code MOOG, and with the moving plasma radiative transfer code, TARDIS. TARDIS code's atomic database was extended to include elements up to 92U with the latest Kurucz line lists with its 2.31 million lines

Relative r-process abundances normalized to the Ba abundance are shown for the sun and two metal-poor stars, CS 22892-05239 and HD88609

Synthetic r-process transmission spectra. The spectra are generated with MOOG. The elements contributing most at the reddest wavelengths are noted in the plot



# Neutron skins and neutron stars in the MMA era

Tidal deformability derived for GW170817 rules out models that predict large stellar radii.

**Fattoyev et al. (see arXiv:1711.06615v2)** infer a corresponding upper limit of about  $R_{\text{skin}}^{208} \leq 0.25$  fm

Tidal deformability  $\Lambda = \frac{2}{3}k_2 \left(\frac{c^2 R}{GM}\right)^5 = \frac{64}{3}k_2 \left(\frac{R}{R_s}\right)^5$  of GW170817 rules out stiff symmetry energy

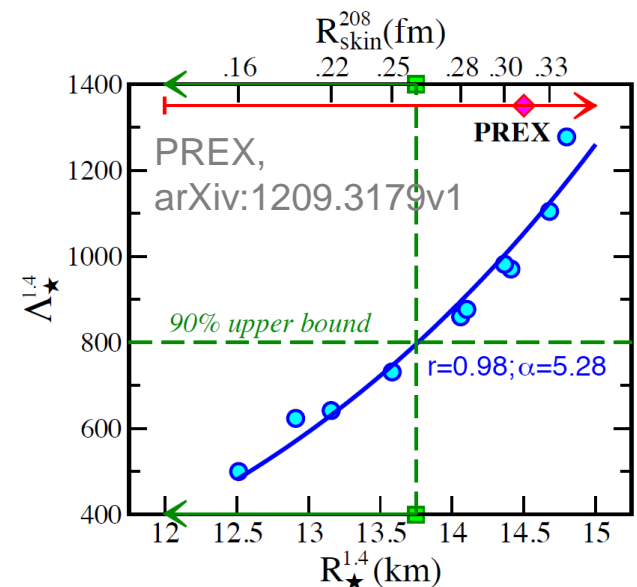
A neutron star having a large radius is much easier to polarize than the corresponding compact star with the same mass but a smaller radius

Nuclear symmetry energy: a quantity that represents the increase in the energy of the system as it departs from the symmetric limit of equal number of neutrons and protons

Despite a difference in length scales of 19 orders of magnitude, the size of a neutron star and the thickness of the neutron skin share a common origin: the pressure of neutron-rich matter. That is, whether pushing against surface tension in an atomic nucleus or against gravity in a neutron star, both the neutron skin and the stellar radius are sensitive to the same EOS

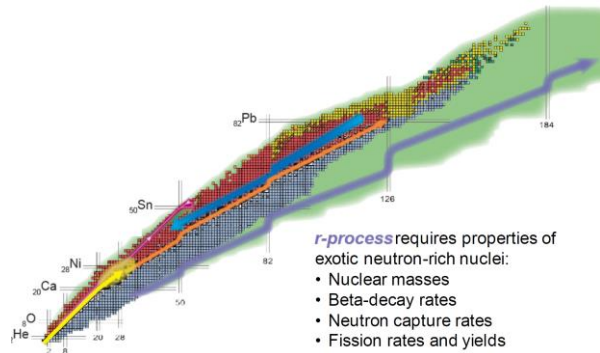
Neutron-skin thickness of  $^{208}\text{Pb}$  is sensitive to the symmetry energy (albeit at a lower density)

If the **upcoming PREX-II experiment** measures a significantly thicker skin, this may be evidence of a softening of the symmetry energy at high densities likely indicative of a phase transition in the interior of neutron stars



# Are long lived superheavy nuclei produced by r-process?

Can we find signatures of superheavy nuclei in kilonova light curves?



“blue remnant”:  $Z < 50$

“red”: lanthanides

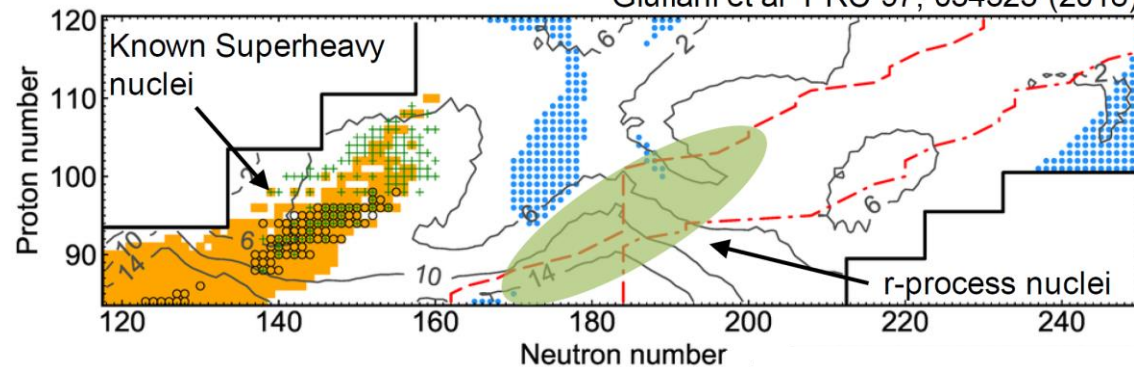
Gabriel Martínez-Pinedo

Joint ApPEC--ECFA--NuPECC Seminar

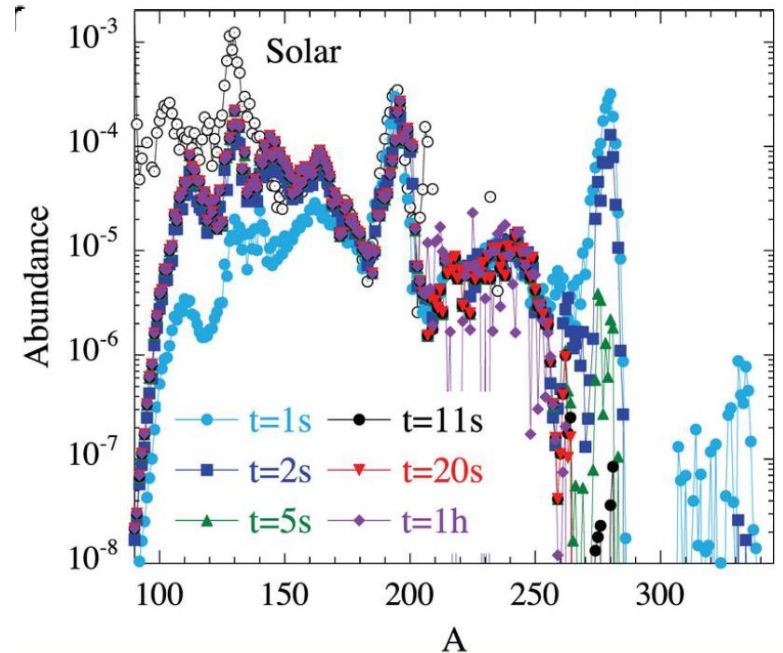
Orsay, France, 14-16 October 2019

Current r-process modes predict substantial production of nuclei around  $A \sim 280$  ( $Z \sim 96$   $N \sim 184$ )  
However during their decay to beta stability they fission on timescales of a few hours

Giuliani et al PRC 97, 034323 (2018)



Requires rapid EM follow-up



# Cosmology



# A new cosmic distance marker

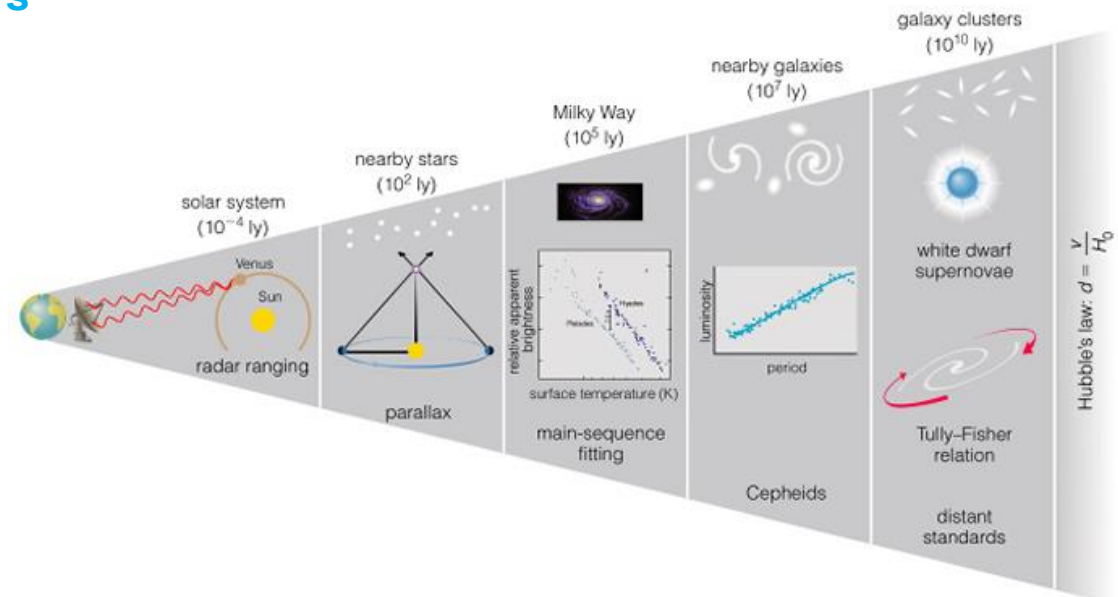
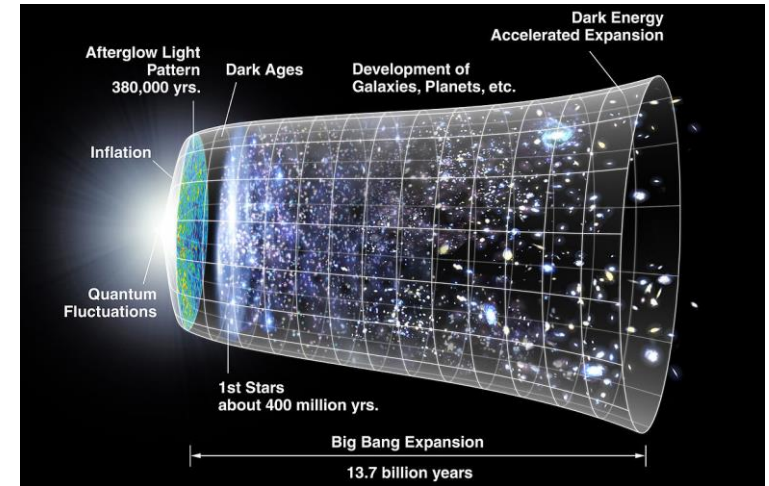
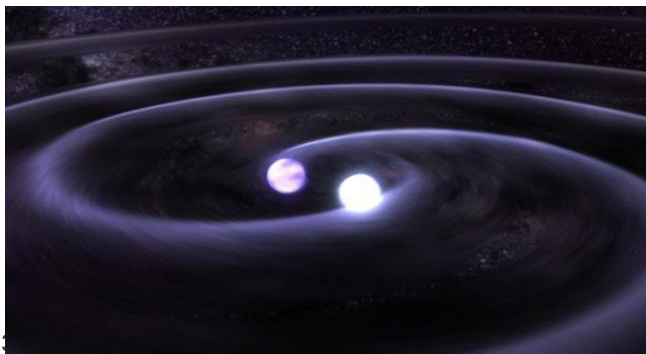
Binary neutron stars allow a new way of mapping out the large-scale structure and evolution of spacetime by comparing distance and redshift

## Current measurements depend on cosmic distance ladder

- Intrinsic brightness of e.g. supernovae determined by comparison with different, closer-by objects
- Possibility of systematic errors at every “rung” of the ladder

## Gravitational waves from binary mergers

Distance can be measured directly from the gravitational wave signal!



# A new cosmic distance marker

A few tens of detections of binary neutron star mergers allow determining the Hubble parameters to about 1-2% accuracy

## Measurement of the local expansion of the Universe

The Hubble constant

- Distance from GW signal
- Redshift from EM counterpart (galaxy NGC 4993)

LIGO+Virgo *et al.*, Nature 551, 85 (2017)

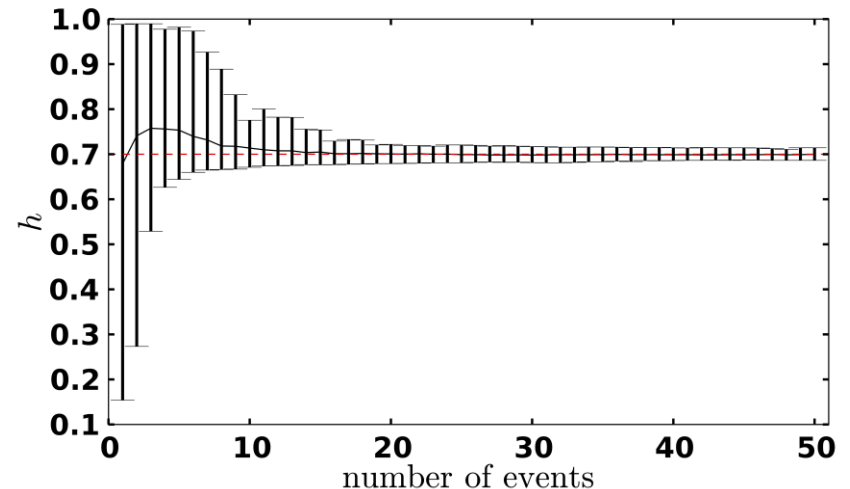
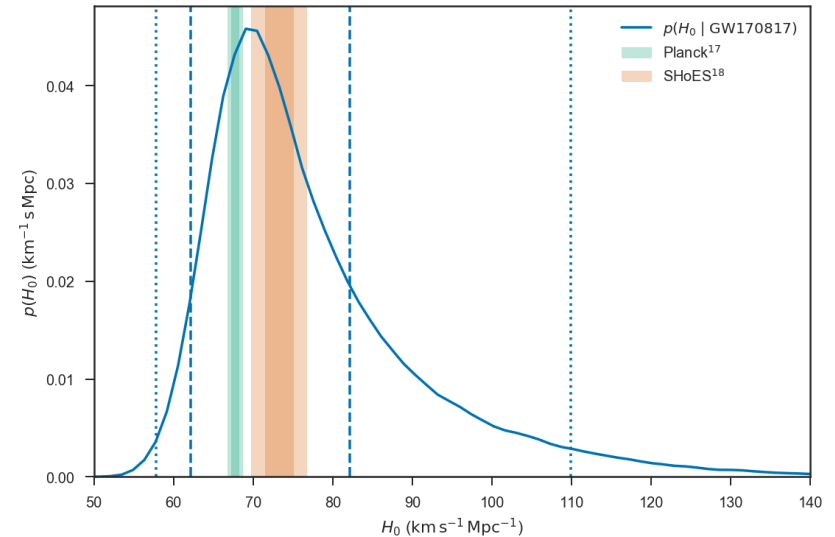
## GW170817

- One detection: limited accuracy
- Few tens of detections with LIGO/Virgo will be needed to obtain O(1-2%) accuracy

Bernard Schutz, Nature 323, 310–311 (1986)

Walter Del Pozzo, PRD 86, 043011 (2012)

Third generation observatories allow studies of the Dark Energy equation of state parameter



# Scientific impact of gravitational wave science

Multi-messenger astronomy started: a broad community is relying on detection of gravitational waves  
Scientific program is limited by the sensitivity of LVC instruments over the entire frequency range

## Fundamental physics

Access to dynamic strong field regime, new tests of General Relativity  
Black hole science: inspiral, merger, ringdown, quasi-normal modes, echo's  
Lorentz-invariance, equivalence principle, polarization, parity violation, axions

## Astrophysics

First observation for binary neutron star merger, relation to sGRB  
Evidence for a kilonova, explanation for creation of elements heavier than iron

## Astronomy

Start of gravitational wave astronomy, population studies, formation of progenitors, remnant studies

## Cosmology

Binary neutron stars can be used as standard “sirens”  
Dark Matter and Dark Energy

## Nuclear physics

Tidal interactions between neutron stars get imprinted on gravitational waves  
Access to equation of state

# April 1, 2019: LIGO and Virgo started observation run O3

Joining O3 is another important step for Virgo



# O3 is here! See <https://gracedb.ligo.org/latest/>

Already 33 (= 41 - 8) public alerts in the 3<sup>rd</sup> science run: more candidates than O1 and O2 combined

Latest — as of 10 October 2019 17:29:34 UTC

Test and MDC events and superevents are not included in the search results by default; see the [query help](#) for information on how to search for events and superevents in those categories.

Query:

Search for:

Search

UID	Labels	t_start	t_0	t_end	FAR (Hz)	Created
<a href="#">S190930t</a>	ADVOK EM_Selected SKYMAP_READY EMBRIGHT_READY PASTRO_READY DQOK GCN_PRELIM_SENT	1253889264.685342	1253889265.685342	1253889266.685342	1.543e-08	2019-09-30 14:34:30 UTC
<a href="#">S190930s</a>	PE_READY ADVOK EM_Selected SKYMAP_READY EMBRIGHT_READY PASTRO_READY DQOK GCN_PRELIM_SENT	1253885758.235347	1253885759.246810	1253885760.253734	3.008e-09	2019-09-30 13:36:04 UTC
<a href="#">S190928c</a>	ADVNO EM_Selected SKYMAP_READY DQOK GCN_PRELIM_SENT	1253671923.328316	1253671923.364500	1253671923.400684	6.729e-09	2019-09-28 02:14:18 UTC
<a href="#">S190924h</a>	PE_READY ADVOK EM_Selected SKYMAP_READY EMBRIGHT_READY PASTRO_READY DQOK GCN_PRELIM_SENT	1253326743.785645	1253326744.846654	1253326745.876674	8.928e-19	2019-09-24 02:19:25 UTC
<a href="#">S190923v</a>	ADVOK EM_Selected SKYMAP_READY EMBRIGHT_READY PASTRO_READY DQOK GCN_PRELIM_SENT	1253278576.645077	1253278577.645508	1253278578.654868	4.783e-08	2019-09-23 12:56:22 UTC
<a href="#">S190915ak</a>	PE_READY ADVOK SKYMAP_READY EMBRIGHT_READY PASTRO_READY DQOK GCN_PRELIM_SENT	1252627039.685111	1252627040.690891	1252627041.730049	9.735e-10	2019-09-15 23:57:25 UTC
<a href="#">S190910h</a>	PE_READY ADVOK SKYMAP_READY EMBRIGHT_READY PASTRO_READY DQOK GCN_PRELIM_SENT	1252139415.544299	1252139416.544448	1252139417.544448	3.584e-08	2019-09-10 08:30:21 UTC
<a href="#">S190910d</a>	PE_READY ADVOK SKYMAP_READY EMBRIGHT_READY PASTRO_READY DQOK GCN_PRELIM_SENT	1252113996.241211	1252113997.242676	1252113998.264918	3.717e-09	2019-09-10 01:26:35 UTC
<a href="#">S190901ap</a>	PE_READY ADVOK SKYMAP_READY EMBRIGHT_READY PASTRO_READY DQOK GCN_PRELIM_SENT	1251415878.837767	1251415879.837767	1251415880.838844	7.027e-09	2019-09-01 23:31:24 UTC
<a href="#">S190829u</a>	PE_READY ADVNO SKYMAP_READY EMBRIGHT_READY PASTRO_READY DQOK GCN_PRELIM_SENT	1251147973.281494	1251147974.283940	1251147975.283940	5.151e-09	2019-08-29 21:06:19 UTC
<a href="#">S190828l</a>	PE_READY ADVOK SKYMAP_READY EMBRIGHT_READY PASTRO_READY DQOK GCN_PRELIM_SENT	1251010526.884921	1251010527.886557	1251010528.913573	4.629e-11	2019-08-28 06:55:26 UTC
<a href="#">S190828j</a>	PE_READY ADVOK SKYMAP_READY EMBRIGHT_READY PASTRO_READY DQOK GCN_PRELIM_SENT	1251009262.739486	1251009263.756472	1251009264.796332	8.474e-22	2019-08-28 06:34:21 UTC
<a href="#">S190822c</a>	ADVNO SKYMAP_READY EMBRIGHT_READY PASTRO_READY DQOK GCN_PRELIM_SENT	1250472616.589125	1250472617.589203	1250472618.589203	6.145e-18	2019-08-22 01:30:23 UTC
<a href="#">S190816i</a>	PE_READY ADVNO SKYMAP_READY EMBRIGHT_READY PASTRO_READY DQOK GCN_PRELIM_SENT	1249995888.757789	1249995889.757789	1249995890.757789	1.436e-08	2019-08-16 13:05:12 UTC
<a href="#">S190814bv</a>	PE_READY ADVOK SKYMAP_READY EMBRIGHT_READY PASTRO_READY DQOK GCN_PRELIM_SENT	1249852255.996787	1249852257.012957	1249852258.021731	2.038e-33	2019-08-14 21:11:18 UTC
<a href="#">S190808ae</a>	ADVNO SKYMAP_READY EMBRIGHT_READY PASTRO_READY DQOK GCN_PRELIM_SENT	1249338098.496141	1249338099.496141	1249338100.496141	3.366e-08	2019-08-08 22:21:45 UTC
<a href="#">S190728q</a>	PE_READY ADVOK SKYMAP_READY EMBRIGHT_READY PASTRO_READY DQOK GCN_PRELIM_SENT	1248331527.497344	1248331528.546797	1248331529.706055	2.527e-23	2019-07-28 06:45:27 UTC
<a href="#">S190727h</a>	PE_READY ADVOK SKYMAP_READY EMBRIGHT_READY PASTRO_READY DQOK GCN_PRELIM_SENT	1248242630.976288	1248242631.985887	1248242633.180176	1.378e-10	2019-07-27 06:03:51 UTC
<a href="#">S190720a</a>	PE_READY ADVOK SKYMAP_READY EMBRIGHT_READY PASTRO_READY DQOK GCN_PRELIM_SENT	1247616533.703127	1247616534.704102	1247616535.860840	3.801e-09	2019-07-20 00:08:53 UTC
<a href="#">S190718v</a>	ADVOK SKYMAP_READY EMBRIGHT_READY PASTRO_READY DQOK GCN_PRELIM_SENT	1247495729.067865	1247495730.067865	1247495731.067865	3.648e-08	2019-07-18 14:35:34 UTC
<a href="#">S190707q</a>	PE_READY ADVOK SKYMAP_READY EMBRIGHT_READY PASTRO_READY DQOK GCN_PRELIM_SENT	1246527223.118398	1246527224.181226	1246527225.284180	5.265e-12	2019-07-07 09:33:44 UTC
<a href="#">S190706ai</a>	PE_READY ADVOK SKYMAP_READY EMBRIGHT_READY PASTRO_READY DQOK GCN_PRELIM_SENT	1246487218.321541	1246487219.344727	1246487220.585938	1.901e-09	2019-07-06 22:26:57 UTC
<a href="#">S190701ah</a>	PE_READY ADVOK SKYMAP_READY EMBRIGHT_READY PASTRO_READY DQOK GCN_PRELIM_SENT	1246048403.576563	1246048404.577637	1246048405.814941	1.916e-08	2019-07-01 20:33:24 UTC
<a href="#">S190630ag</a>	PE_READY ADVOK SKYMAP_READY EMBRIGHT_READY PASTRO_READY DQOK GCN_PRELIM_SENT	1245955942.175325	1245955943.179550	1245955944.183184	1.435e-13	2019-06-30 18:52:28 UTC
<a href="#">S190602ag</a>	PE_READY ADVOK SKYMAP_READY EMBRIGHT_READY PASTRO_READY DQOK GCN_PRELIM_SENT	1243533584.081266	1243533585.089355	1243533586.346191	1.901e-09	2019-06-02 17:59:51 UTC
<a href="#">S190524q</a>	ADVNO SKYMAP_READY EMBRIGHT_READY PASTRO_READY DQOK GCN_PRELIM_SENT	1242708743.678669	1242708744.678669	1242708746.133301	6.971e-09	2019-05-24 04:52:30 UTC
<a href="#">S190521r</a>	PE_READY ADVOK SKYMAP_READY EMBRIGHT_READY PASTRO_READY DQOK GCN_PRELIM_SENT	1242459856.453418	1242459857.460739	1242459858.642090	3.168e-10	2019-05-21 07:44:22 UTC
<a href="#">S190521q</a>	PE_READY ADVOK SKYMAP_READY EMBRIGHT_READY PASTRO_READY DQOK GCN_PRELIM_SENT	1242442966.447266	1242442967.606934	1242442968.888184	3.801e-09	2019-05-21 03:02:49 UTC
<a href="#">S190519bj</a>	PE_READY ADVOK SKYMAP_READY EMBRIGHT_READY PASTRO_READY DQOK GCN_PRELIM_SENT	1242315361.378873	1242315362.655762	1242315363.676270	5.702e-09	2019-05-19 15:36:04 UTC
<a href="#">S190518bb</a>	ADVNO SKYMAP_READY EMBRIGHT_READY PASTRO_READY DQOK GCN_PRELIM_SENT	1242242376.474609	1242242377.474609	1242242380.922655	1.004e-08	2019-05-18 19:19:39 UTC
<a href="#">S190517h</a>	PE_READY ADVOK SKYMAP_READY EMBRIGHT_READY PASTRO_READY DQOK GCN_PRELIM_SENT	1242107478.819517	1242107479.994141	1242107480.994141	2.373e-09	2019-05-17 05:51:23 UTC
<a href="#">S190513bm</a>	PE_READY ADVOK SKYMAP_READY EMBRIGHT_READY PASTRO_READY DQOK GCN_PRELIM_SENT	1241816085.736106	1241816086.869141	1241816087.869141	3.734e-13	2019-05-13 20:54:48 UTC
<a href="#">S190512at</a>	PE_READY ADVOK SKYMAP_READY EMBRIGHT_READY PASTRO_READY DQOK GCN_PRELIM_SENT	1241719651.411441	1241719652.416286	1241719653.518066	1.901e-09	2019-05-12 18:07:42 UTC
<a href="#">S190510q</a>	ADVOK SKYMAP_READY EMBRIGHT_READY PASTRO_READY DQOK GCN_PRELIM_SENT	1241492396.291636	1241492397.291636	1241492398.293185	8.834e-09	2019-05-10 03:00:03 UTC
<a href="#">S190503bf</a>	PE_READY ADVOK SKYMAP_READY EMBRIGHT_READY PASTRO_READY DQOK GCN_PRELIM_SENT	1240944861.288574	1240944862.412598	1240944863.422852	1.636e-09	2019-05-03 18:54:26 UTC
<a href="#">S190426c</a>	PE_READY ADVOK SKYMAP_READY EMBRIGHT_READY PASTRO_READY DQOK GCN_PRELIM_SENT	1240327332.331168	1240327333.348145	1240327334.353516	1.947e-08	2019-04-26 15:22:15 UTC
<a href="#">S190425z</a>	ADVOK SKYMAP_READY EMBRIGHT_READY PASTRO_READY DQOK	1240215502.011549	1240215503.011549	1240215504.018242	4.538e-13	2019-04-25 08:18:26 UTC
<a href="#">S190421ar</a>	PE_READY ADVOK SKYMAP_READY EMBRIGHT_READY PASTRO_READY DQOK GCN_PRELIM_SENT	1239917953.250977	1239917954.409180	1239917955.409180	1.489e-08	2019-04-21 21:39:16 UTC
<a href="#">S190412m</a>	PE_READY ADVOK SKYMAP_READY EMBRIGHT_READY PASTRO_READY DQOK GCN_PRELIM_SENT	1239082261.146717	1239082262.222168	1239082263.229492	1.683e-27	2019-04-12 05:31:03 UTC
<a href="#">S190408an</a>	PE_READY ADVOK SKYMAP_READY EMBRIGHT_READY PASTRO_READY DQOK GCN_PRELIM_SENT	1238782699.268296	1238782700.287958	1238782701.359863	2.811e-18	2019-04-08 18:18:27 UTC
<a href="#">S190405ar</a>	ADVNO SKYMAP_READY EMBRIGHT_READY PASTRO_READY DQOK	1238515307.863646	1238515308.863646	1238515309.863646	2.141e-04	2019-04-05 16:01:56 UTC

# O3 event candidates and O1 + O2 detections versus run time

Already 33 (= 41 - 8) public alerts in the 3<sup>rd</sup> science run: more candidates than O1 and O2 combined

**Number of candidates:** 41 (excluding retractions)

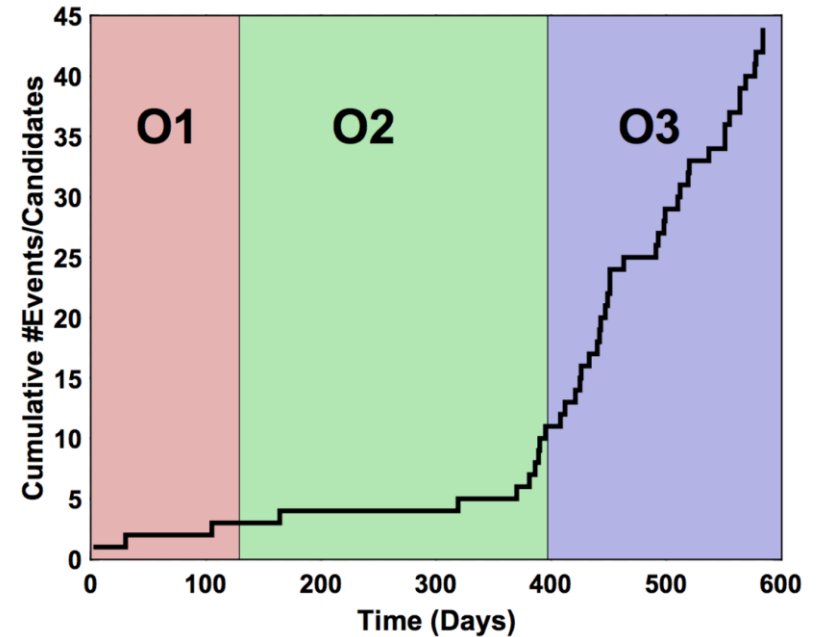
**False alarm rate (FAR)**

26 with FAR > 1/100 yr and 15 with FAR < 1/100 yr

Number of retractions: 8

**Candidate types**

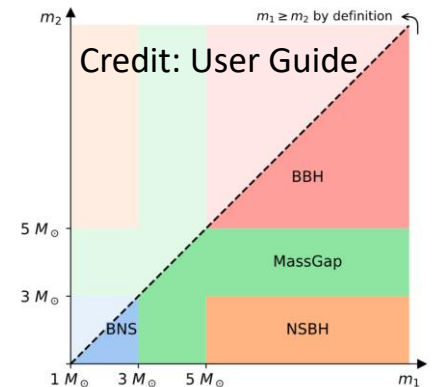
21 BBH, 3 BNS, 2 Mass Gap, 4 NSBH, 3 Terrestrial



Expected number of events for O3 (i.e. 1 calendar year of running)

SNR > 4 in at least two detectors and network SNR 12

Observation Run	Network	Expected BNS Detections	Expected NSBH Detections	Expected BBH Detections
O3	HLV	$2_{-2}^{+8}$	$0_{-0}^{+19}$	$15_{-10}^{+19}$



# BNS event candidates

Three candidates have significant astrophysical probability of being a BNS event

For BNS and NSBH candidates extensive multi-wavelength campaign but no significant EM counterparts

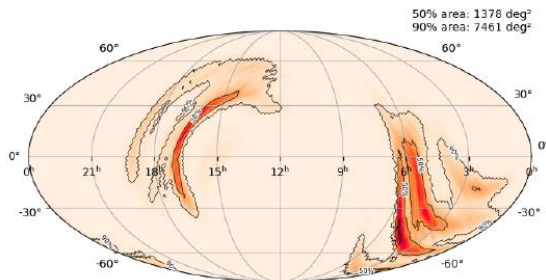
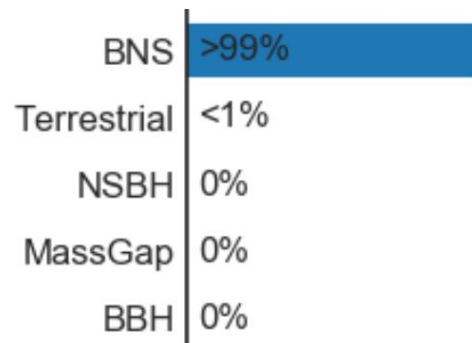
## S190425z

FAR < 1/100 yrs

7461 deg<sup>2</sup> in 90% c.r.

Distance  $156 \pm 41$  Mpc

L, V



GCN 24168, 24228

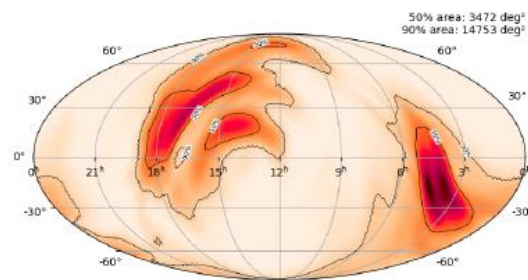
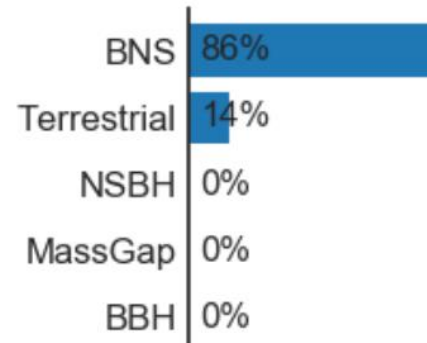
## S190901ap

FAR: 1 in 4.5 yrs

14753 deg<sup>2</sup>

$241 \pm 79$  Mpc

L, V



25606, 25614

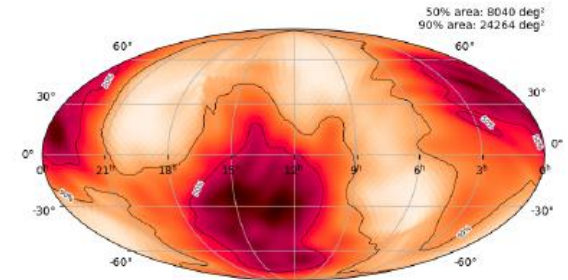
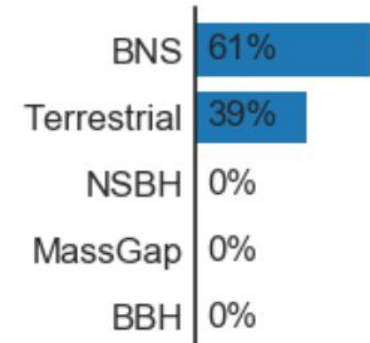
## S190910h

FAR: 1.13 per year

24264 deg<sup>2</sup>

$230 \pm 88$  Mpc

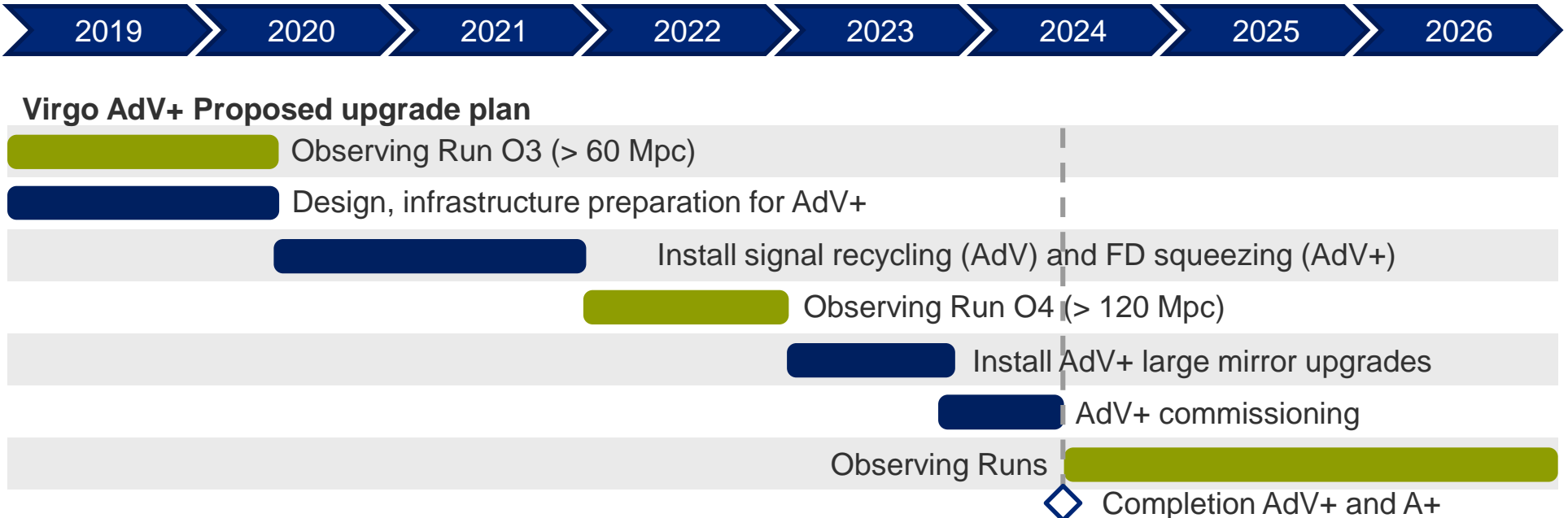
L



25707, 25778

# Scheduling issues

Five year plan: substrates must be ordered in 2020



Commissioning break in October 2019

Duration of O3: until the end of April 2020 (duration of O4 has not been decided)

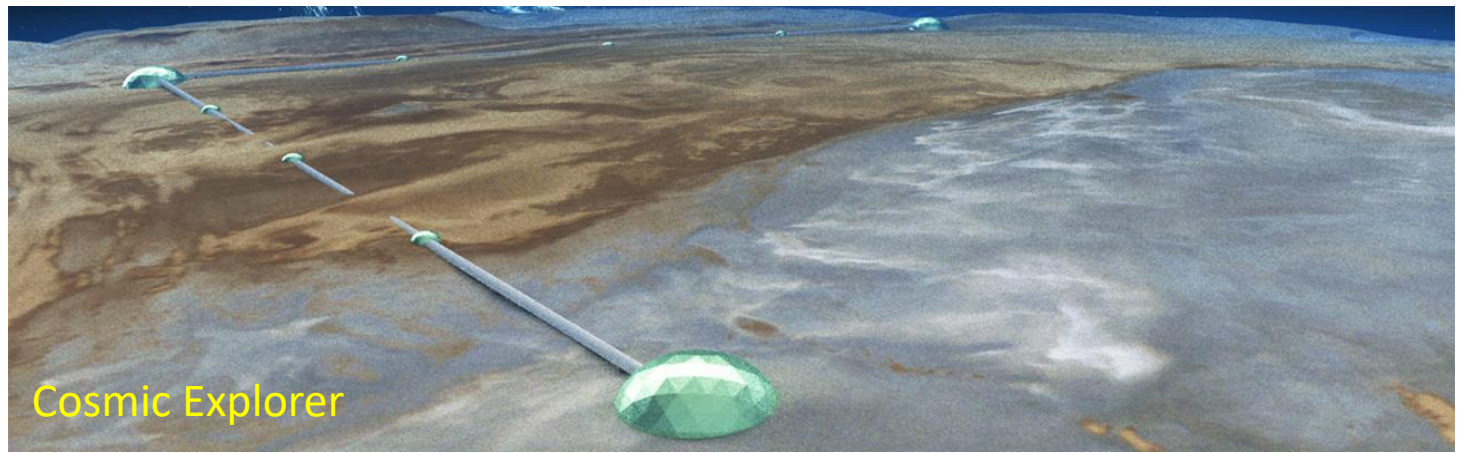
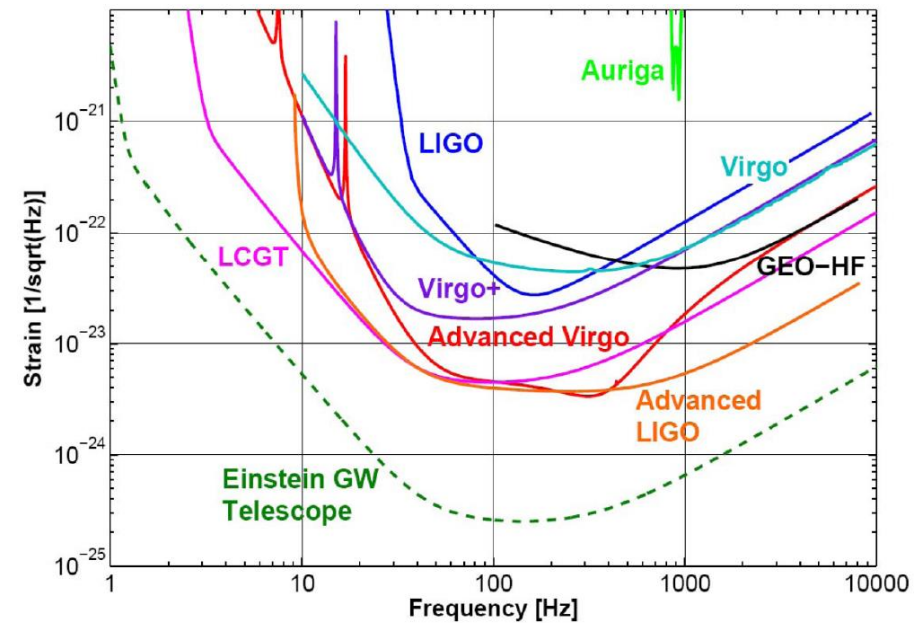
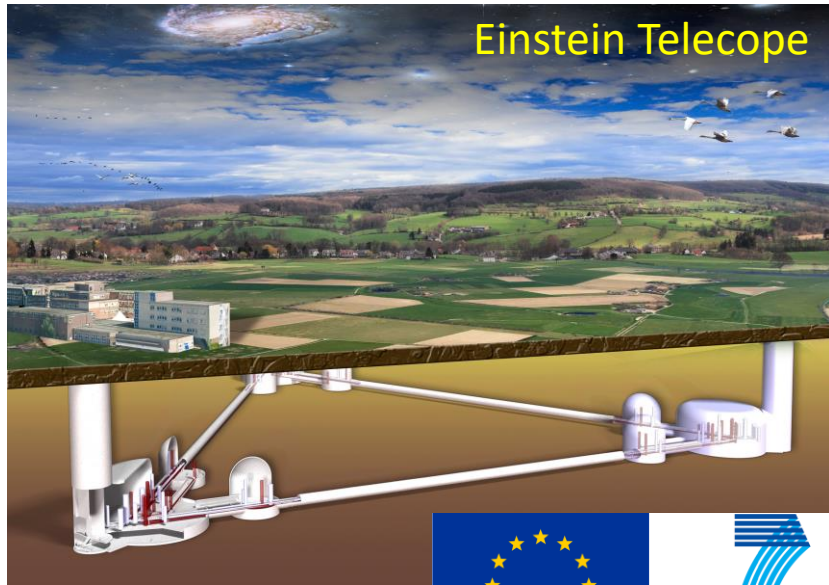
Break between O3 and O4 around 20 months (allowing for installation and commissioning)

AdV+ to be carried out in parallel with LIGO's A+ upgrade

AdV+ is part of a strategy to go from 2nd generation to Einstein Telescope

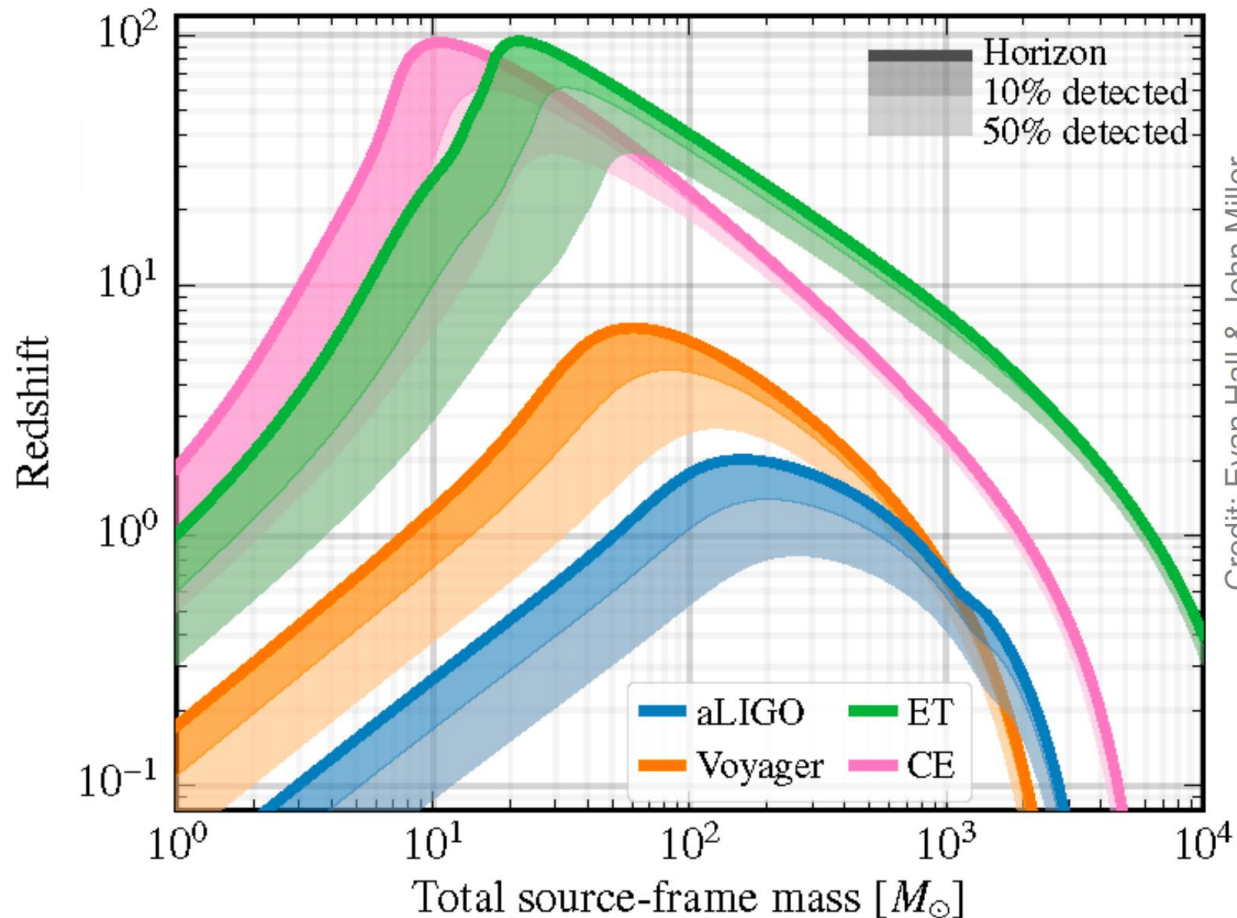
# Einstein Telescope and Cosmic Explorer

Realizing the next gravitational wave observatories is a coordinated effort with US to create a worldwide 3G network



# Einstein Telescope and Cosmic Explorer

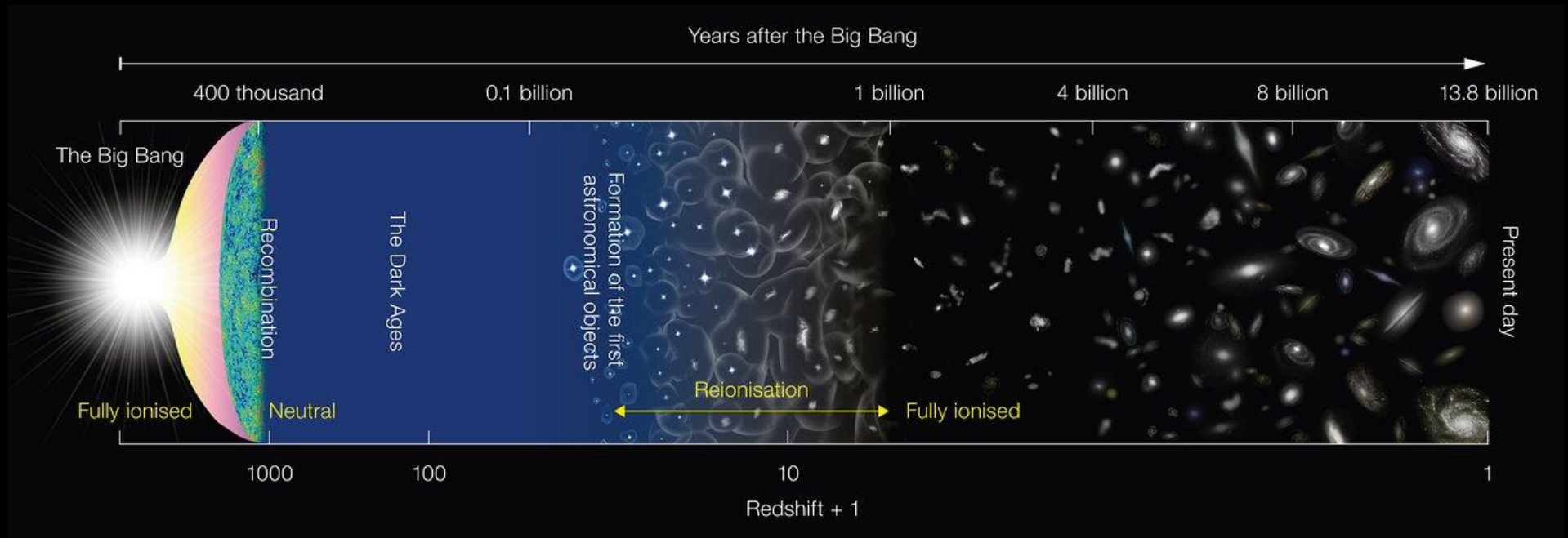
Einstein Telescope will feature excellent low-frequency sensitivity and have great discovery potential



For science case, see <https://www.dropbox.com/s/gihpzcue4qd92dt/science-case.pdf?dl=0>

# Einstein Telescope

Einstein Telescope can observe BBH mergers to red shifts of about 100. This allows a new approach to cosmography. Study primordial black holes, BH from population III stars (first metal producers), etc.



Einstein Telescope has direct access to signals from black hole mergers in this range

# Bright future for gravitational wave research

LIGO and Virgo are operational. KAGRA in Japan joins this year, LIGO-India under construction. ESA launches LISA in 2034. Einstein Telescope and CE CDRs financed. Strong support by APPEC

## Gravitational wave research

- LIGO and Virgo operational
- KAGRA to join this year
- LIGO-India under construction (2025)
- ESA selects LISA, NASA rejoins
- Pulsar Timing Arrays, such as EPTA and SKA
- Cosmic Microwave Background radiation

## Einstein Telescope and Cosmic Explorer

- CDR ET financed by EU in FP7, CE by NSF
- APPEC gives GW a prominent place in the new Roadmap and especially the realization of ET

## Next steps for 3G

- Organize the community and prepare a credible plan for EU funding agencies
- ESFRI Roadmap (2020)
- Support 3G: <http://www.et-gw.eu/index.php/letter-of-intent>

